



**HAL**  
open science

## Complete finite-strain isotropic thermo-elasticity

Paul Bouteiller

► **To cite this version:**

Paul Bouteiller. Complete finite-strain isotropic thermo-elasticity. *European Journal of Mechanics - A/Solids*, 2023, 100, pp.105017. 10.1016/j.euromechsol.2023.105017 . hal-04109554

**HAL Id: hal-04109554**

**<https://hal.science/hal-04109554>**

Submitted on 30 May 2023

**HAL** is a multi-disciplinary open access archive for the deposit and dissemination of scientific research documents, whether they are published or not. The documents may come from teaching and research institutions in France or abroad, or from public or private research centers.

L'archive ouverte pluridisciplinaire **HAL**, est destinée au dépôt et à la diffusion de documents scientifiques de niveau recherche, publiés ou non, émanant des établissements d'enseignement et de recherche français ou étrangers, des laboratoires publics ou privés.

# Complete finite-strain isotropic thermo-elasticity

Paul Bouteiller<sup>a,b</sup>

<sup>a</sup>CEA, DAM, DIF, F-91297 Arpajon, France

<sup>b</sup>Université Paris-Saclay, CEA, Laboratoire Matière en Conditions Extrêmes, F-91680 Bruyères-le-Châtel, France

---

## Abstract

This paper deals with finite strain isotropic thermo-elasticity without any specific Ansatz regarding the Helmholtz free energy. On the theoretical side, an Eulerian setting of isotropic thermo-elasticity is developed, based on the objective left Cauchy-Green tensor along with the Cauchy stress. The construction of the elastic model relies on a particular invariants choice of the strain measure. These invariants are built so that a succession of elementary experiments, in which the invariants evolve independently, ensures the complete identification of the Helmholtz free energy and thus of the thermo-elastic constitutive law. Expressions idealizing these experimental tests are proposed. A wide range of hyperelastic models are found to be a special case of the model proposed herein.

*Keywords:* Finite strain thermo-elasticity, experimental identification

---

## Introduction

Elasticity is probably one of the most extensively discussed topics in the analytical mechanics literature over the last few centuries. Since Robert Hooke's linear relationship linking the current Cauchy stress  $\boldsymbol{\sigma}$  to the linearized strain  $\boldsymbol{\varepsilon}$ , many authors studied small strain but also non-linear elasticity, the latter being well suited to study materials, such as polymer, which undergo large deformations. The fundamental ground of this phenomenon, which can precede more complex non linear events, is now a very well assessed subject, both theoretically [3, 9, 25] and experimentally.

However, specific Ansatz are still commonly used concerning the Helmholtz free energy from which the elastic constitutive law is derived. Classical small-strain elasticity, linking the second Piola-Kirchhoff tensor  $\boldsymbol{\pi}$  to the right Green-Lagrange strain tensor  $\boldsymbol{E}$  relies on a quadratic expansion of the Helmholtz free energy with respect to the small strain  $\boldsymbol{E}$ . As regards finite strain elasticity, where such series expansion are no longer valid, the construction is based on a choice of the Helmholtz free energy according to invariants of the deformation tensor. Two main categories are often distinguished, depending on the state variables

---

*Email address:* paul.bouteiller@cea.fr (Paul Bouteiller)

21 chosen. On the one hand, Neo-Hookean[20], Mooney-Rivlin [22], or Yeoh [36] models postulate a polynomial  
 22 expansion of the free energy with respect to the fundamental invariants of a strain tensor. The coefficients  
 23 involved in the polynomial expansion are fitted to reproduce experimental data. On the other hand, stretched  
 24 based models, such as Ogden’s which develop the Helmholtz free energy as a power series, retain the positive  
 25 eigenvalues of the right Cauchy-Green tensor  $\mathbf{C}$ . Ogden models have been found to be very efficient for large  
 26 strain elasticity of rubber like material [6]. Many articles have offered reviews of these different models and  
 27 their respective pros and cons [7, 10, 19, 23].

28 The first objective of this paper is to present a choice of a triplet of kinematically significant invariants,  
 29 allowing for the rigorous identification of the Helmholtz free energy, through a succession of simple elementary  
 30 experiments and without *a posteriori* adjustment. These invariants are chosen so that they can evolve  
 31 independently.

32 In Section 1, we will recall the main lines of construction of the finite strain isotropic thermo-elastic  
 33 behavior. In Section 2, we will present the invariants of the left Cauchy-Green deformation tensor used for  
 34 the construction of the elastic model and the resulting constitutive law. Then, we will study, Section 3, the  
 35 successive elementary experiments which allow the identification of the Helmholtz free energy. Physically  
 36 realistic expressions for the experimental data required to build the model will then be proposed in Section  
 37 4.

## 38 1. Reminder of finite strain elasticity

39 This section briefly presents the fundamental assumption of finite strain isotropic thermo-elasticity within  
 40 an Eulerian setting. The formulation of the general theory is given in the thermodynamic framework by  
 41 introducing the Helmholtz free energy as a function of a finite strain measure, and by exploring both the  
 42 first and the second law of thermodynamics.

### 43 1.1. Framework

44 Let  $\mathcal{D}_0^m \in \mathbb{R}^3$  be a material domain corresponding to the reference configuration of a continuous medium.  
 45 Particles labeled by  $\mathbf{x}_0 \in \mathcal{D}_0^m$  are transported in the current configuration to  $\mathbf{x}_t \in \mathcal{D}_t^m$  by a one-to-one  
 46 mapping  $\varphi_t$ . Let us note  $\mathbf{F}$  the deformation gradient of this mapping.

47 Let us consider two observers (reference frames)  $\mathcal{R}$  and  $\tilde{\mathcal{R}}$ . We denote  $\mathbf{Q}_0$  the orthogonal transformation  
 48 linking these two reference frames at the initial time and  $\mathbf{Q}_t$  the orthogonal tensor linking these same two  
 49 observers in the current configuration. A second-rank tensor,  $\mathbf{Y}$  for the observer  $\mathcal{R}$ , equal to  $\tilde{\mathbf{Y}}$  for the  
 50 observer  $\tilde{\mathcal{R}}$ , is called invariant (or “objective Lagrangian”) [21] if:

$$\tilde{\mathbf{Y}} = \mathbf{Q}_0 \cdot \mathbf{Y} \cdot \mathbf{Q}_0^\top \quad \mathbf{Q}_0 \in SO(3); \forall t. \quad (1)$$

51 Similarly, we will call “objective” any second-rank tensor  $\mathbf{X}$  satisfying the following equality:

$$\tilde{\mathbf{X}} = \mathbf{Q}_t \cdot \mathbf{X} \cdot \mathbf{Q}_t^\top \quad \mathbf{Q}_t \in SO(3). \quad (2)$$

52 The invariance or objectivity property of a tensor is intrinsic and comes either from its mathematical  
 53 definition or from a physically motivated assumption. The first step in the construction of a constitutive  
 54 law is the choice of a deformation measure, which cannot be simply  $\mathbf{F}$ , among two large families:

- 55 • On the one hand, strain tensors based on the product  $\mathbf{C} = \mathbf{F}^\top \cdot \mathbf{F}$  or its related tensors of the form  
 56  $\mathbf{Y} = \frac{1}{n}(\mathbf{U}^n - \mathbf{1})$  with  $\mathbf{U} = \sqrt{\mathbf{C}}$  (pure stretch). These deformation tensors are often called “right  
 57 strain measure”, “Lagrangian” or “invariant” because they obey the relation (1). These strain measures  
 58 are used to close the mechanical problem by relating the first or second Piola-Kirchoff stress tensor  $\mathbf{P}$ ,  
 59  $\boldsymbol{\pi}$  (which are also postulate invariant) to the displacement field  $\mathbf{u}$ .
- 60 • On the other hand, strain measure, called “left”, “Eulerian” or “objective”, and based on the left Cauchy-  
 61 Green deformation  $\mathbf{B} = \mathbf{F} \cdot \mathbf{F}^\top$  (subsequently called “Finger tensor”) are more rarely considered to  
 62 build elasticity models. These deformation measurements effectively link the objective Cauchy stress  
 63  $\boldsymbol{\sigma}$  to the displacement field.

## 64 1.2. Elastic behavior

65 The finite-strain isotropic elastic behavior is based on the following three assertions:

- 66 1. Temperature and a strain measure are the only state variables.
- 67 2. The stress measure is a state function.
- 68 3. In all evolutions, the intrinsic dissipation is null.

69 The first assumption 1) forbids the presence of additional internal variables which could be the witness of  
 70 phenomena such as plasticity, damage etc... But also anisotropy through a structural tensor [4, 37]. The  
 71 second assumption 2) excludes viscous effects and a possible strain rate  $\mathbf{D}$  ( $\mathbf{D}$  denotes the symmetric part of  
 72 the spatial velocity gradient) dependency of the Cauchy stress. The last assumption 3) ensures reversibility  
 73 in the sense that the entropy production other than thermal is zero. To satisfy these three requirements,  
 74 most treatises devote the so-called “Lagrangian” approaches and relate the second Piola-Kirchoff tensor to  
 75 the right Green-Lagrange deformation tensor. Eulerian formulations of elasticity are rarely considered (see  
 76 nevertheless [24, 31]), especially since the Cauchy stress cannot be written as the simple derivative of a  
 77 potential with respect to a strain measure.

78 *1.3. Eulerian finite strain isotropic elasticity*

79 Here, we choose to catch the motion with the left Cauchy-Green objective strain tensor  $\mathbf{B}$  which we  
80 relate to the Cauchy stress  $\boldsymbol{\sigma}$  whose physical meaning is perfectly clear.

81  
82 The isotropy of the material  $\boldsymbol{\sigma}(T, \mathbf{B}) = \mathbf{Q}_t \cdot \boldsymbol{\sigma} \cdot \mathbf{Q}_t^\top(T, \mathbf{Q}_t \cdot \mathbf{B} \cdot \mathbf{Q}_t^\top)$  and the Rivlin-Ericksen theorem [25]  
83 implies that the Cauchy stress necessarily expands as a quadratic polynomial of the strain measure:

$$\boldsymbol{\sigma} = K_0^B \mathbf{1} + K_1^B \mathbf{B} + K_2^B \mathbf{B}^2. \quad (3)$$

84 The coefficients  $K_i^B$  are scalar functions of the temperature, but also of a triplet of  $\mathbf{B}$  invariants. Their  
85 expressions, as a function of the free energy, can be deduced from the nullity of the intrinsic dissipation (see  
86 [35] p.295) written on the current (spatial) configuration:

$$\Phi = -\rho \left( \dot{\psi}^m + \dot{T}s^m \right) + \boldsymbol{\sigma} : \mathbf{D} = 0. \quad (4)$$

87 For an isotropic material, the Helmholtz massic free energy is an isotropic function [4, 32]  $\psi^m(T, \mathbf{B}) =$   
88  $\psi^m(T, \mathbf{Q}_t \cdot \mathbf{B} \cdot \mathbf{Q}_t^\top)$ ,  $\forall \mathbf{Q}_t \in SO(3)$  so that there exists  $f_\psi^B$  such that:

$$\psi^m(T, \mathbf{B}) = f_\psi^B(T, B_I, B_{II}, B_{III}), \quad (5)$$

89 where the fundamental invariants  $(B_I, B_{II}, B_{III})$  denote the coefficients of the characteristic polynomial of  $\mathbf{B}$   
90 (*main invariant*). Note that any other triplet of invariants bijectively related to  $(B_I, B_{II}, B_{III})$ , is legitimate.  
91 Thus, the ‘‘principal’’ invariants defined by  $B_i = \frac{1}{i} \text{Tr} \mathbf{B}^i$  are often used to construct elastic laws as their  
92 partial derivatives with respect to the strain measure are straightforward. In the following, we will retain  
93 invariants whose kinematic meaning is clear.

94 According to the fundamental invariants  $(B_I, B_{II}, B_{III})$ , the isotropic finite strain thermo-elastic law  
95 reads, (see Appendix A but also [16, 31]):

$$\boldsymbol{\sigma} = \frac{2\rho_0}{\sqrt{B_{III}}} \left( B_{III} \partial_{B_{III}} f_\psi^B \mathbf{1} + (\partial_{B_I} f_\psi^B + B_I \partial_{B_{II}} f_\psi^B) \mathbf{B} - \partial_{B_{II}} f_\psi^B \mathbf{B}^2 \right). \quad (6)$$

96 *1.4. Elastic model based on volumetric split*

Most materials exhibit completely different volumetric and isochoric responses so that we make use of  
the isochoric-volumetric commutative split of the gradient  $\mathbf{F}$  [13, 30]:

$$\mathbf{F} = \left( J^{\frac{1}{3}} \mathbf{1} \right) \cdot \left( J^{-\frac{1}{3}} \mathbf{F} \right) = \left( J^{\frac{1}{3}} \mathbf{1} \right) \cdot \bar{\mathbf{F}}, \quad (7)$$

$$\Rightarrow \mathbf{B} = \left( J^{\frac{2}{3}} \mathbf{1} \right) \cdot \left( J^{-\frac{2}{3}} \mathbf{B} \right) = \mathbf{B}^{sph} \cdot \bar{\mathbf{B}}. \quad (8)$$

97  $\mathbf{B}^{sph}$  is a spherical tensor whose only invariant is the volume expansion  $J$ :

$$J = \det \mathbf{F} = \sqrt{\det \mathbf{B}} = \sqrt{B_{III}}. \quad (9)$$

98 The isochoric Finger tensor  $\bar{\mathbf{B}}$  satisfies  $\det \bar{\mathbf{B}} = 1$  and is therefore represented by two invariants. We  
 99 note, without any ambiguity,  $\bar{B}_I$  and  $\bar{B}_{II}$  the two fundamental invariants of the isochoric Finger tensor.  
 100 These invariants are trivially related to those of  $\mathbf{B}$  by:

$$\bar{B}_I = J^{-\frac{2}{3}} B_I = B_{III}^{-\frac{1}{3}} B_I \text{ and } \bar{B}_{II} = J^{-\frac{4}{3}} B_{II} = B_{III}^{-\frac{2}{3}} B_{II}. \quad (10)$$

101 One can find a function  $\tilde{f}_\psi^B$  of the invariants  $(T, \bar{B}_I, \bar{B}_{II}, B_{III})$  coinciding with the Helmholtz massic free  
 102 energy:

$$\psi^m(T, \mathbf{B}) = f_\psi^B(T, B_I, B_{II}, B_{III}) = \tilde{f}_\psi^B(T, \bar{B}_I, \bar{B}_{II}, B_{III}). \quad (11)$$

103 The partial derivatives of the new function  $\tilde{f}_\psi^B$  are then obtained by simple algebraic calculations. The  
 104 elastic law (6) is then transformed to give (see Appendix B):

$$\begin{aligned} \boldsymbol{\sigma} &= \frac{2\rho_0}{\sqrt{B_{III}}} \left( B_{III} \partial_{B_{III}} \tilde{f}_\psi^B \mathbf{1} + \partial_{\bar{B}_I} \tilde{f}_\psi^B \mathbf{Dev} \bar{\mathbf{B}} - \partial_{\bar{B}_{II}} \tilde{f}_\psi^B \mathbf{Dev} (\bar{\mathbf{B}}^2 - \text{Tr}(\bar{\mathbf{B}}) \bar{\mathbf{B}}) \right), \\ \boldsymbol{\sigma} &= \frac{2\rho_0}{\sqrt{B_{III}}} \left( B_{III} \partial_{B_{III}} \tilde{f}_\psi^B \mathbf{1} + \frac{\partial_{\bar{B}_I} \tilde{f}_\psi^B}{B_{III}^{\frac{1}{3}}} \mathbf{Dev} \mathbf{B} - \frac{\partial_{\bar{B}_{II}} \tilde{f}_\psi^B}{B_{III}^{\frac{2}{3}}} \mathbf{Dev} (\mathbf{B}^2 - \text{Tr}(\mathbf{B}) \mathbf{B}) \right). \end{aligned} \quad (12)$$

105  $\mathbf{Dev} \mathbf{X} = \mathbf{X} - (\frac{1}{3} \text{Tr} \mathbf{X}) \mathbf{1}$  refers to the deviatoric (trace-less) part of a second-order tensor.

106 (12) emphasizes the deep link between the *isochoric strain* and the *deviatoric part of the stress*.

## 107 2. Construction of the thermo-elastic model

108 The invariants used so far are natural, but inefficient for the identification of the Helmholtz free energy,  
 109 as they evolve simultaneously in classical experimental tests. The corner-stone of the subsequent section is  
 110 the choice of independent invariants associated with simple elementary experiments, allowing them to evolve  
 111 one after the other.

### 112 2.1. State variables

113 *First invariant of the isochoric Finger tensor.* We introduce a first invariant  $\gamma_s$  of the isochoric Finger tensor  
 114  $\bar{\mathbf{B}}$ , defined by:

$$\gamma_s = \sqrt{\bar{B}_I - 3} = \sqrt{\frac{B_I}{B_{III}^{\frac{1}{3}}} - 3}, \quad (13)$$

115  $\gamma_s$  is bijectively related to the maximum distortion  $\delta_{\max}$  (see [15]):

$$\gamma_s = \sqrt{3} \sqrt{(\delta_{\max})^{\frac{2}{3}} - 1} \text{ with } \delta_{\max} = \max_{\mathbf{Q} \in SO(3)} \frac{1}{|\det(\mathbf{Q} \cdot \mathbf{u}_t, \mathbf{Q} \cdot \mathbf{u}'_t, \mathbf{Q} \cdot \mathbf{u}''_t)|}, \quad (14)$$

116 where  $(\mathbf{u}_t, \mathbf{u}'_t, \mathbf{u}''_t)$  denotes an initially orthogonal material direction triplet (at  $t = 0$ ,  $\det(\mathbf{u}_0, \mathbf{u}'_0, \mathbf{u}''_0) = 1$ ).

117 The maximum distortion  $\delta_{\max}$  reflects the maximum decrease of the solid angle formed by three initially

118 orthogonal material directions. Moreover, in an isochoric simple shear test, defined by the transformation  
 119 field (see Figure 1):

$$\mathbf{x}_t = \boldsymbol{\varphi}(\mathbf{x}_0, t) = J^{\frac{1}{3}}(\mathbf{x}_0 + \gamma Y \mathbf{e}_x), \quad (15)$$

simple algebra yield  $\gamma_s = \gamma$ , so that  $\gamma_s$  equalized the motion magnitude.

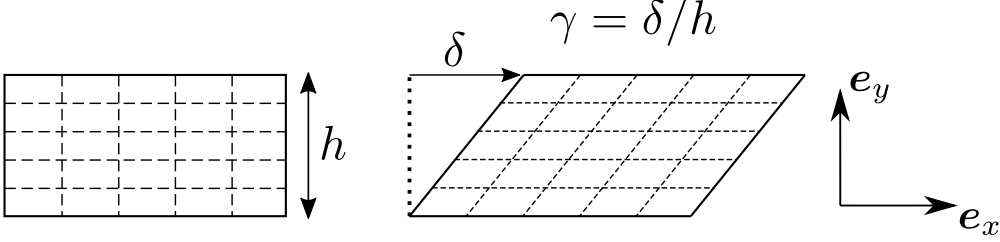


Figure 1: Isochoric planar simple shear kinematics

120

121 *Second invariant of the isochoric Finger tensor.* We propose to construct a second invariant of  $\bar{\mathbf{B}}$  which  
 122 remains null in any isochoric simple shear test. Thus, one may clarify the dependence of the Helmholtz  
 123 massic free energy with respect to this new invariant. The isochoric Finger tensor associated with the  
 124 motion (15) reads:

$$\bar{\mathbf{B}} = (1 + \gamma^2)(\mathbf{e}_x \otimes \mathbf{e}_x) + \gamma(\mathbf{e}_x \otimes \mathbf{e}_y + \mathbf{e}_y \otimes \mathbf{e}_x) + \mathbf{e}_y \otimes \mathbf{e}_y + \mathbf{e}_z \otimes \mathbf{e}_z. \quad (16)$$

125 Set  $\gamma_{\perp} = 0$  and  $e = 1$  in (D.3) shows that the two fundamentals invariants of (16) stay equal  $\bar{B}_{\text{II}} = \bar{B}_{\text{I}}$ .

126 We define the invariant  $\gamma_t$ , identically zero in any spherical evolution and in a simple shear test, by:

$$\gamma_t = \sqrt{\bar{B}_{\text{I}} - 3} - \sqrt{\bar{B}_{\text{II}} - 3} = \gamma_s - \sqrt{\frac{\bar{B}_{\text{II}}}{J^{\frac{4}{3}}} - 3}, \quad (17)$$

127  $\gamma_t$  is always well defined (i.e. the terms under the roots are always positive) by concavity of the logarithm.

128 A closed form of its variations' domain is given in Appendix C.

## 129 2.2. Constitutive law with the new invariants set

130 The list of reduced state variables retained is thus  $(T, J, \gamma_s, \gamma_t)$  (9), (13), (17). The relations are inversed  
 131 in:

$$J = B_{\text{III}}^{\frac{1}{2}}; \quad \gamma_s = \sqrt{\bar{B}_{\text{I}} - 3}; \quad \gamma_t = \gamma_s - \sqrt{\bar{B}_{\text{II}} - 3} \Leftrightarrow B_{\text{III}} = J^2; \quad \bar{B}_{\text{I}} = \gamma_s^2 + 3; \quad \bar{B}_{\text{II}} = (\gamma_s - \gamma_t)^2 + 3; \quad (18)$$

132 The generic elastic law (12), expressed in terms of the principal invariants  $(T, \bar{B}_{\text{I}}, \bar{B}_{\text{II}}, B_{\text{III}})$  is transformed  
 133 by applying the chain rule:

$$\boldsymbol{\sigma} = \rho_0 \left( \partial_J \tilde{f}_{\psi} \mathbf{1} + \frac{1}{\gamma_s J^{\frac{5}{3}}} \left( \partial_{\gamma_s} \tilde{f}_{\psi} + \partial_{\gamma_t} \tilde{f}_{\psi} \right) \text{Dev} \mathbf{B} + \frac{\partial_{\gamma_t} \tilde{f}_{\psi}}{(\gamma_s - \gamma_t) J^{\frac{7}{3}}} \text{Dev} (\mathbf{B}^2 - \text{Tr}(\mathbf{B})\mathbf{B}) \right). \quad (19)$$

134 This is the most general isotropic thermo-elastic law, formulated with respect to the variables  $(T, J, \gamma_s, \gamma_t)$ .  
 135 Postulating that the free energy does not depend on the  $\gamma_t$  invariant, i.e.  $\partial_{\gamma_t} \tilde{f}_\psi = 0$ , reduces (19) to the  
 136 elastic law used by [24, 26, 29, 31]. It should be noted, however, that in these papers, the expression  
 137 of the free energy is presented as a hypothesis and is not deduced from experimentally assessed stresses.  
 138 These models, being limited to the triplet  $(T, J, \gamma_s)$ , choose not to distinguish energetically two different  
 139 deformations which would share the same maximum distortion  $\delta_{\max}$  and thus the same invariant  $\gamma_s$ .

### 140 3. Experimental identification

141 The thermodynamic construction presented herein follows the generic method presented by Guarrigues  
 142 [16, 17].

143 Let  $\tilde{f}_\psi$  denote the free energy variation within the non-isothermal thermo-elastic process from a reference  
 144 configuration,  $E_0 = (T_0, 1, 0, 0)$  for which the free energy is set to zero, to an arbitrary configuration given  
 145 by the state variables  $(T, J, \gamma_s, \gamma_t)$ :

$$\psi^m = \tilde{f}_\psi(T, J, \gamma_s, \gamma_t). \quad (20)$$

To define the Helmholtz massic free energy at any point  $(T, J, \gamma_s, \gamma_t)$  of the state space, we define a particular path

$$E_0 = (T_0, 1, 0, 0) \xrightarrow{\mathcal{P}^{(1)}} E_1 = (T, 1, 0, 0) \xrightarrow{\mathcal{P}^{(2)}} E_2 = (T, J, 0, 0) \xrightarrow{\mathcal{P}^{(3)}} E_3 = (T, J, \gamma_s, 0) \xrightarrow{\mathcal{P}^{(4)}} E_t = (T, J, \gamma_s, \gamma_t)$$

146 such that  $\tilde{f}_\psi$  is additively found, given the energy variation in every path:

$$\psi^m = g^{(1)}(T) + g^{(2)}(T, J) + g^{(3)}(T, J, \gamma_s) + g^{(4)}(T, J, \gamma_s, \gamma_t). \quad (21)$$

147 -  $g^{(1)}(T)$  is the Helmholtz massic free energy variation within  $\mathcal{P}^{(1)}$  (strain-locked heating):

$$\dot{T} \neq 0; \quad J = 1; \quad \dot{J} = 0; \quad \gamma_s = 0; \quad \dot{\gamma}_s = 0; \quad \gamma_t = 0; \quad \dot{\gamma}_t = 0; \quad (22)$$

148 -  $g^{(2)}(T, J)$  is the Helmholtz massic free energy variation within  $\mathcal{P}^{(2)}$  (isothermal spherical motion):

$$\dot{T} = 0; \quad \dot{J} \neq 0; \quad \gamma_s = 0; \quad \dot{\gamma}_s = 0; \quad \gamma_t = 0; \quad \dot{\gamma}_t = 0; \quad (23)$$

149 -  $g^{(3)}(T, J, \gamma_s)$  is the Helmholtz massic free energy variation within  $\mathcal{P}^{(3)}$  (isochoric simple shear test):

$$\dot{T} = 0; \quad \dot{J} = 0; \quad \dot{\gamma}_s \neq 0; \quad \gamma_t = 0; \quad \dot{\gamma}_t = 0; \quad (24)$$

150 -  $g^{(4)}(T, J, \gamma_s, \gamma_t)$  is the Helmholtz massic free energy variation within  $\mathcal{P}^{(4)}$  (isothermal isochoric iso-  
 151 trace motion):

$$\dot{T} = 0; \quad \dot{J} = 0; \quad \dot{\gamma}_s = 0; \quad \dot{\gamma}_t \neq 0; \quad (25)$$

152 with the initial conditions:

$$g^{(1)}(T_0) = 0; \quad g^{(2)}(T, 1) = 0, \quad \forall T; \quad g^{(3)}(T, J, 0) = 0, \quad \forall (T, J); \quad g^{(4)}(T, J, \gamma_s, 0) = 0, \quad \forall (T, J, \gamma_s); \quad (26)$$

153 which leads to cancel the following partial derivatives:

$$\begin{aligned} \partial_T g^{(2)}(T, 1) &= 0; \quad \partial_T g^{(3)}(T, J, 0) = \partial_J g^{(3)}(T, J, 0) = 0 \quad \forall T, J; \\ \partial_T g^{(4)}(T, J, \gamma_s, 0) &= \partial_J g^{(4)}(T, J, \gamma_s, 0) = \partial_{\gamma_s} g^{(4)}(T, J, \gamma_s, 0) = 0 \quad \forall T, J, \gamma_s. \end{aligned} \quad (27)$$

154 The general form of the massic entropy is given by the Helmholtz relation:

$$s^m = -\partial_T \tilde{f}_\psi = -\partial_T g^{(1)} - \partial_T g^{(2)} - \partial_T g^{(3)} - \partial_T g^{(4)}. \quad (28)$$

155 The massic internal energy is deduced from the definition of the Helmholtz free energy:

$$e^m = \tilde{f}_\psi + T s^m = g^{(1)} + g^{(2)} + g^{(3)} + g^{(4)} - T(\partial_T g^{(1)} + \partial_T g^{(2)} + \partial_T g^{(3)} + \partial_T g^{(4)}). \quad (29)$$

### 156 3.1. Elementary evolutions

157 The identification of the four unknown functions  $g^{(1)}(T)$ ,  $g^{(2)}(T, J)$ ,  $g^{(3)}(T, J, \gamma_s)$  and  $g^{(4)}(T, J, \gamma_s, \gamma_t)$   
158 comes down to experimental measures in a few experiments carried under the following ideal experimental  
159 conditions:

160 1) body forces are negligible;

161 2) state variables  $(T, J, \gamma_s, \gamma_t)$  are uniform across the specimen.

162 3) experimental data are evaluated in a quasi-static setting so that the kinetic energy can be neglected;

163  $g^{(1)}(T)$  will be determined by a simple energy balance whereas direct integration of experimental stress data  
164 shall clarify the rest of the Helmholtz free energy.

#### 165 3.1.1. Strain-locked pure heating

166 The first evolution  $\mathcal{P}^{(1)}$  is a pure heating, strain locked, experiment:  $\mathbf{B} = \mathbf{1}$ ,  $J = 1$ ,  $\dot{J} = 0$ ,  $\gamma_s = 0$ ,  
167  $\dot{\gamma}_s = 0$ ,  $\gamma_t = 0$ ,  $\dot{\gamma}_t = 0$ . We measure the algebraic massic heat  $q_{exp}^{m(1)}(T)$  supplied to the system to go from  $T_0$   
168 to  $T$ . The conservation of energy between the states  $E_0$  and  $E_1$  is written (quasi-static evolution:  $\Delta e_c^m = 0$ ,  
169 no deformation:  $w^{m ext} = 0$ ):

$$e_1^m - \underbrace{e_0^m}_0 = q_{exp}^{m(1)}(T), \quad (30)$$

which leads to the differential equation in  $g^{(1)}$  from (29):

$$\begin{aligned} g^{(1)}(T) - T(\partial_T g^{(1)}(T) + \partial_T g^{(2)}(T, 1) + \partial_T g^{(3)}(T, 1, 0)) + \partial_T g^{(4)}(T, 1, 0, 0) &= q_{exp}^{m(1)}(T), \\ \Leftrightarrow g^{(1)}(T) - T \partial_T g^{(1)}(T) &= q_{exp}^{m(1)}(T) \quad \text{see (27),} \\ \Leftrightarrow g^{(1)}(T) &= -T \int_{T_0}^T \frac{q_{exp}^{m(1)}(\tilde{T})}{\tilde{T}^2} d\tilde{T}. \end{aligned} \quad (31)$$

170 This experimental measurement is very difficult to perform, especially when the samples tend to contract  
 171 (usually during cooling). We will see later, Section 3.1.5, that this ideal experiment can be replaced by a  
 172 free thermal expansion followed by an isothermal spherical motion.

### 173 3.1.2. Spherical motion

174 In the second path  $\mathcal{P}^{(2)}$ , the deformation is purely spherical ( $\mathbf{B} = J^{\frac{2}{3}}\mathbf{1}$ ,  $\gamma_s = 0$ ,  $\dot{\gamma}_s = 0$ ,  $\gamma_t = 0$ ,  $\dot{\gamma}_t = 0$ )  
 175 and isothermal ( $\dot{T} = 0$ ). The elastic law (19) proves that stress tensor must also be spherical:

$$\boldsymbol{\sigma}^{(2)} = \rho_0 \partial_J \tilde{f}_\psi \mathbf{1}, \quad (32)$$

176 and is thus completely characterized by its mean stress.

177 In this experiment, we measure the pressure  $p_{exp}^{(2)}(T, J)$  which is the opposite of the uniform normal stress  
 178 applied on the boundary if the hypothesis 2) p.8 holds:

$$p_{exp}^{(2)}(T, J) = -\frac{\text{Tr}\boldsymbol{\sigma}^{(2)}}{3} = -\rho_0 \partial_J g^{(2)}(T, J) \quad \text{see (27)}. \quad (33)$$

179 The second contribution to the Helmholtz massic free energy variation then follows naturally.

$$g^{(2)}(T, J) = -\frac{1}{\rho_0} \int_1^J p_{exp}^{(2)}(T, \tilde{J}) d\tilde{J}. \quad (34)$$

180 In the shock-wave mechanics community, the determination of this pressure with respect to the volumetric  
 181 change (or equivalently to the mass density  $\rho$ ) and the temperature, is often referred to as the “equation of  
 182 state (EOS)” [1].

### 183 3.1.3. Isochoric iso- $T$ planar simple shear test

184 To perform an isochoric isothermal planar simple shear [18] in the  $(\mathbf{e}_x, \mathbf{e}_y)$  plane with an initial volume  
 185 expansion  $J$ , we impose the following position field on the particles:

$$\mathbf{x}_t = J^{\frac{1}{3}}(\mathbf{x}_0 + \gamma Y \mathbf{e}_x), \quad (35)$$

186 where  $\mathbf{x}_0 = X\mathbf{e}_x + Y\mathbf{e}_y + Z\mathbf{e}_z$  is the reference position of a particle. The Finger tensor  $\mathbf{B} = \mathbf{F} \cdot \mathbf{F}^\top$  in the  
 187 orthonormal basis  $(\mathbf{e}_x, \mathbf{e}_y, \mathbf{e}_z)$  for this isochoric motion have already been given (16). The strain tensor is  
 188 uniform in the specimen  $\partial_{\mathbf{x}_0} \mathbf{B} = \mathbf{0}$  so that  $\gamma_s$  is uniform as well and satisfies:  $\gamma_s = \sqrt{\overline{B}_I - 3} = \sqrt{\gamma^2} = \pm\gamma$ .

189 *Stress tensor in the  $\mathcal{P}^{(3)}$  evolution.* The general thermo-elastic law reads:

$$\boldsymbol{\sigma} = \rho_0 \left( \partial_J \tilde{f}_\psi \mathbf{1} + \frac{1}{\gamma_s J^{\frac{5}{3}}} \left( \partial_{\gamma_s} \tilde{f}_\psi + \partial_{\gamma_t} \tilde{f}_\psi \right) \text{Dev} \mathbf{B} + \frac{\partial_{\gamma_t} \tilde{f}_\psi}{(\gamma_s - \gamma_t) J^{\frac{7}{3}}} \text{Dev} (\mathbf{B}^2 - \text{Tr}(\mathbf{B})\mathbf{B}) \right). \quad (36)$$

190 Given the equalities  $\gamma_t = 0$ ,  $\partial_{\gamma_s} g^{(4)}(T, J, \gamma_s, 0) = 0$ , simple calculations show that the tangential stress  
 191  $\tau_{exp}^{(3)}(T, J, \gamma_s) = \sigma_{12}^{(3)}$  within this evolution is directly related to  $\partial_{\gamma_s} g^{(3)}$  by:

$$\tau_{exp}^{(3)} = \frac{\rho_0}{J} \partial_{\gamma_s} g^{(3)}(T, J, \gamma_s). \quad (37)$$

192 In this experiment, we measure the tangential stress  $\tau_{exp}^{(3)}$  as a function of  $\gamma$  and we deduce by a simple  
 193 integration the value of the function  $g^{(3)}$ :

$$g^{(3)} = \frac{J}{\rho_0} \int_0^{\gamma_s} \tau_{exp}^{(3)}(T, J, \gamma) d\gamma. \quad (38)$$

#### 194 3.1.4. Iso- $\gamma_s$ iso- $T$ isochoric double shear test

195  $\mathcal{P}^{(4)}$  is an isothermal, isochoric, iso- $\gamma_s$  experiment. Several tests grants this triple condition. For the  
 196 sake of simplicity, we introduce herein the “double shear test”, eventhough this experiment does not scan  
 197 the whole domain of variation of  $\gamma_t$ . In the Appendix D, we will present a wider two-parameter test family,  
 198 which include the present “double shear experiment”, and which browse the whole domain for the variable  
 199  $\gamma_t$ .

200 *Isochoric double shear test.* Consider the motion defined by the following transformation (see also Figure  
 2):

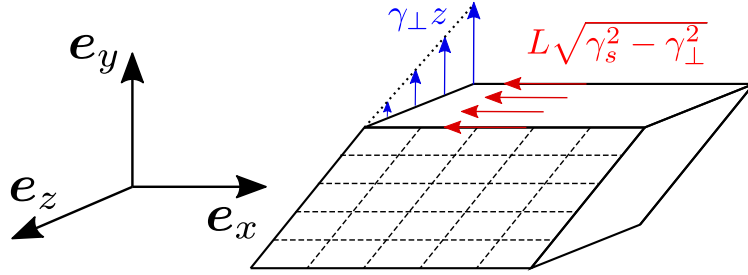


Figure 2: Double shear kinematic

$$201 \quad \mathbf{x}_t = J^{\frac{1}{3}} (\mathbf{x}_0 + \sqrt{\gamma_s^2 - \gamma_{\perp}^2} Y \mathbf{e}_x + \gamma_{\perp} Z \mathbf{e}_y), \quad (39)$$

202 where  $\mathbf{x}_0 = X \mathbf{e}_x + Y \mathbf{e}_y + Z \mathbf{e}_z$  is the reference position of a particle,  $J$  is the volume dilatation prior from  
 203 path  $\mathcal{P}^{(2)}$  and constant in path  $\mathcal{P}^{(3)}$  and  $\mathcal{P}^{(4)}$ ,  $\gamma_s$  is the slip prior from path  $\mathcal{P}^{(3)}$  and constant in path  
 204  $\mathcal{P}^{(4)}$ . The components of the Finger tensor  $\mathbf{B} = \mathbf{F} \cdot \mathbf{F}^{\top}$  in the orthonormal basis  $\{\mathbf{e}_x, \mathbf{e}_y, \mathbf{e}_z\}$  for this  
 205 isochoric motion are:

$$\mathbf{F} = J^{\frac{1}{3}} \begin{pmatrix} 1 & \sqrt{\gamma_s^2 - \gamma_{\perp}^2} & 0 \\ 0 & 1 & \gamma_{\perp} \\ 0 & 0 & 1 \end{pmatrix} \Rightarrow \overline{\mathbf{B}} = \begin{pmatrix} 1 + \gamma_s^2 - \gamma_{\perp}^2 & \sqrt{\gamma_s^2 - \gamma_{\perp}^2} & 0 \\ \sqrt{\gamma_s^2 - \gamma_{\perp}^2} & 1 + \gamma_{\perp}^2 & \gamma_{\perp} \\ 0 & \gamma_{\perp} & 1 \end{pmatrix} \Rightarrow \overline{B}_I = \gamma_s^2 + 3. \quad (40)$$

206 This test continuously shifts the deformation from a simple shear test in the  $(\mathbf{e}_x, \mathbf{e}_y)$  plane to the same state  
 207 in the  $(\mathbf{e}_y, \mathbf{e}_z)$  plane while keeping the first invariant  $\gamma_s$  constant.

208 *Stress tensor in the double shear test.* Injecting the strain measure deduced from (39) in (36), one can see that  
 209 the out of plane shear stress  $\sigma_{13}^{(4)}$  is directly related to the derivative of the Helmholtz massic free energy with

210 respect to  $\gamma_t$ . Indeed,  $\bar{B}_{13}^2$  given by (D.2) and (36) proves that the tangential stress  $\tau_{exp}^{(4)}(T, J, \gamma_s, \gamma_t) = \sigma_{13}^{(4)}$   
 211 in this evolution equalized:

$$\begin{aligned} \tau_{exp}^{(4)}(T, J, \gamma_s, \gamma_\perp) &= \frac{\rho_0}{J(\gamma_s - \gamma_t)} \partial_{\gamma_t} g^{(4)}(T, J, \gamma_s, \gamma_t) \gamma_\perp \sqrt{\gamma_s^2 - \gamma_\perp^2} \text{ with } \gamma_t = \gamma_s - \sqrt{\gamma_s^2 + \gamma_\perp^2 (\gamma_s^2 - \gamma_\perp^2)} \text{ see (D.9),} \\ \tau_{exp}^{(4)}(T, J, \gamma_s, \gamma_t) &= \frac{\rho_0}{J(\gamma_s - \gamma_t)} \partial_{\gamma_t} g^{(4)}(T, J, \gamma_s, \gamma_t) \sqrt{(\gamma_s - \gamma_t)^2 - \gamma_s^2}. \end{aligned} \quad (41)$$

212 The expression for the massic free energy  $g^{(4)}$  is obtained once more by integrating the experimental data:

$$g^{(4)}(T, J, \gamma_s, \gamma_t) = \frac{J}{\rho_0} \int_0^{\gamma_t} \frac{\gamma_s - \tau}{\sqrt{(\gamma_s - \tau)^2 - \gamma_s^2}} \tau_{exp}^{(4)}(T, J, \gamma_s, \tau) d\tau. \quad (42)$$

213 When  $\gamma_\perp$  evolves in the interval  $\left[0, \frac{\gamma_s}{\sqrt{2}}\right]$ , the invariant  $\gamma_t$  takes its values in  $\gamma_t \in \left[\gamma_s \left(1 - \sqrt{1 + \frac{\gamma_s^2}{4}}\right), 0\right]$   
 214 (see Appendix D).

215 Note that this out-of-plane shear-stress  $\sigma_{13}^{(4)}$  is purely “non-linear” in the sense that it arises from the  
 216 quadratic term of the strain measure, therefore, it cannot be predicted by any “linearized” versions of the  
 217 elastic law or by any model neglecting the contribution of the second strain invariant  $\bar{B}_{II}$ .

218  
 219 The “double shear experiment” is not a standard laboratory test but can be performed using an efficient  
 220 hexapod machine (Stewart machine [11, 34]).

### 221 3.1.5. Free thermal expansion ( $\mathcal{P}^{(5)}$ )

222 A direct measurement of the massic heat  $q_{exp}^{m(1)}$  in the first path  $\mathcal{P}^{(1)}$  (strain-locked heating) is rather  
 223 difficult. This experiment can be replaced by a free-stress thermal expansion ( $p_{exp}^{(2)}(T, J_{exp}^{(5)}(T)) = 0, \forall T$ ),  
 224 followed by an isothermal spherical deformation which brings the volume expansion  $J_{exp}^{(5)}(T)$  back to 1.

225  
 Writing the conservation of energy for this evolution between the initial state  $(T_0, 1, 0, 0)$  and the freely  
 expanded state  $(T, J_{exp}^{(5)}, 0, 0)$ , it follows:  $e_5^m = q_{exp}^{m(5)}(T)$ . Moreover, the massic internal energy in the freely  
 expanded state  $(T, J_{exp}^{(5)}, 0, 0)$  is also given by (29):

$$e_5^m = q_{exp}^{m(1)}(T) - \frac{1}{\rho_0} \int_1^{J_{exp}^{(5)}} p_{exp}^{(2)}(T, \tilde{J}) - T \partial_T p_{exp}^{(2)}(T, \tilde{J}) d\tilde{J}, \quad (43)$$

$$\Rightarrow q_{exp}^{m(1)}(T) = q_{exp}^{m(5)}(T) + \frac{1}{\rho_0} \int_1^{J_{exp}^{(5)}} p_{exp}^{(2)}(T, \tilde{J}) - T \partial_T p_{exp}^{(2)}(T, \tilde{J}) d\tilde{J}. \quad (44)$$

226 (44) proves that given the experimental pressure  $p_{exp}^2(T, J)$  and the free-stress expansion massic heat  
 227  $q_{exp}^{m(5)}(T)$ , one may determine  $q_{exp}^{m(1)}(T)$ . The function (31) is then finally written:

$$g^{(1)}(T) = -T \int_{T_0}^T \frac{q_{exp}^{m(5)}(\tilde{T})}{\tilde{T}^2} d\tilde{T} - \frac{T}{\rho_0} \int_{T_0}^T \left( \int_1^{J_{exp}^{(5)}(\tilde{T})} p_{exp}^{(2)}(\tilde{T}, \tilde{J}) - \tilde{T} \partial_{\tilde{T}} p_{exp}^{(2)}(\tilde{T}, \tilde{J}) d\tilde{J} \right) d\tilde{T}. \quad (45)$$

228 *3.2. Synthesis*

229 The complete identification of the finite strain thermo-elastic model relies on four experimental data:

230 1)  $q_{exp}^{m(1)}(T)$ : massic heat exchanged in the first path  $\mathcal{P}^{(1)}$  (strain-locked heating or cooling), with the  
231 condition:

$$q_{exp}^{m(1)}(T_0) = 0. \quad (46)$$

232 2)  $p_{exp}^{(2)}(T, J)$ : pressure in the spherical evolution  $\mathcal{P}^{(2)}$  (isothermal spherical deformation), with the con-  
233 dition:

$$p_{exp}^{(2)}(T, 1) = p_{exp}^{(1)}(T), \forall T. \quad (47)$$

234 3)  $\tau_{exp}^{(3)}(T, J, \gamma_s)$ : in-plane shear stress in the isochoric planar shear test  $\mathcal{P}^{(3)}$ , along with the condition:

$$\tau_{exp}^{(3)}(T, J, 0) = 0, \forall T \forall J. \quad (48)$$

235 4)  $\tau_{exp}^{(4)}(T, J, \gamma_s, \gamma_t)$ : out-of-plane tangential stress in the fourth path  $\mathcal{P}^{(4)}$ , with the condition:

$$\tau_{exp}^{(4)}(T, J, \gamma_s, 0) = 0, \forall T \forall J \forall \gamma_s. \quad (49)$$

$g^{(1)}, g^{(2)}, g^{(3)}, g^{(4)}$  which determine the state functions are expressed in terms of these measurements:

$$g^{(1)}(T) = -T \int_{T_0}^T \frac{q_{exp}^{m(1)}(\tilde{T})}{\tilde{T}^2} d\tilde{T} \text{ or (45),} \quad (50)$$

$$g^{(2)}(T, J) = -\frac{1}{\rho_0} \int_1^J p_{exp}^{(2)}(T, \tilde{J}) d\tilde{J}, \quad (51)$$

$$g^{(3)}(T, J, \gamma_s) = \frac{J}{\rho_0} \int_0^{\gamma_s} \tau_{exp}^{(3)}(T, J, \gamma) d\gamma, \quad (52)$$

$$g^{(4)}(T, J, \gamma_s, \gamma_t) = \frac{J}{\rho_0} \int_0^{\gamma_t} \frac{\gamma_s - \tau}{\sqrt{(\gamma_s - \tau)^2 - \gamma_s^2}} \tau_{exp}^{(4)}(T, J, \gamma_s, \tau) d\tau. \quad (53)$$

236 The internal massic energy is assumed to be a state function, as to ensure (29) takes a simpler expression:

$$e^m = q_{exp}^{m(1)} + g^{(2)} - T \partial_T g^{(2)} + g^{(3)} - T \partial_T g^{(3)} + g^{(4)} - T \partial_T g^{(4)}. \quad (54)$$

237 For the numerical assessment of the model, it is not necessary to compute explicitly  $g^{(1)}$  because this function  
238 does not appear neither in the constitutive law, nor in the internal energy.

239 *3.3. Volumetric/isochoric splitting assumption*

As already mentioned, hyperelastic materials exhibit radically different volume and shear behavior. This explains a well-accepted splitting of the Helmholtz free energy with respect to the isochoric/volumetric part of the strain tensor (see [24, 27]). In this section, we emphasize that this partition comes down to a very

natural assertion: the pressure remains unchanged in isochoric evolutions. With the previous results, the pressure in any state  $(T, J, \gamma_s, \gamma_t)$  is:

$$\begin{aligned} -\frac{\text{Tr}\boldsymbol{\sigma}}{3} &= -\rho_0 \partial_J \left( g^{(2)}(T, J) + g^{(3)}(T, J, \gamma_s) + g^{(4)}(T, J, \gamma_s, \gamma_t) \right) \\ &= p_{exp}^{(2)}(T, J) + \int_0^{\gamma_s} \tau_{exp}^{(3)}(T, J, \gamma_s) - J \partial_J \tau_{exp}^{(3)}(T, J, \gamma_s) d\gamma \\ &\quad - \int_0^{\gamma_t} \frac{\gamma_s - \tau}{\sqrt{(\gamma_s - \tau)^2 - \gamma_s^2}} \left( \tau_{exp}^{(4)} + J \partial_J \tau_{exp}^{(4)} \right) (T, J, \gamma_s, \tau) d\tau. \end{aligned} \quad (55)$$

The pressure in any state is a function of the tangential stresses  $\tau_{exp}^{(3)}$ ,  $\tau_{exp}^{(4)}$  measured during the paths  $\mathcal{P}^{(3)}$ ,  $\mathcal{P}^{(4)}$ . If one performs the  $\mathcal{P}^{(3)}$  experiment from the initial state ( $p_{exp}^{(2)}(T_0, 1) = 0$ , no prior volume expansion), the Cauchy stress tensor generated is not deviatoric.

**Hypothesis** Optional Simplification. *In isochoric deformation, the pressure does not vary. Both conditions  $\partial_{\gamma_t} \text{Tr}\boldsymbol{\sigma} = 0$ ,  $\partial_{\gamma_s} \text{Tr}\boldsymbol{\sigma} = 0$  and (55) lead to the differential equations:*

$$\begin{aligned} \tau_{exp}^{(4)} + J \partial_J \tau_{exp}^{(4)} = 0 &\Rightarrow \tau_{exp}^{(4)}(T, J, \gamma_s, \gamma_t) = \frac{\hat{\tau}_{exp}^{(4)}(T, \gamma_s, \gamma_t)}{J}, \\ \tau_{exp}^{(3)} + J \partial_J \tau_{exp}^{(3)} = 0 &\Rightarrow \tau_{exp}^{(3)}(T, J, \gamma_s) = \frac{\hat{\tau}_{exp}^{(3)}(T, \gamma_s)}{J}. \end{aligned} \quad (56)$$

Inserting these expressions into the general formula (52)–(53), (56) obviously split the Helmholtz free energy into an isochoric/volumetric contributions:

$$\psi^m(T, J, \gamma_s, \gamma_t) = g^{(1)}(T) + g^{(2)}(T, J) + g^{(3)}(T, \gamma_s) + g^{(4)}(T, \gamma_s, \gamma_t). \quad (57)$$

This assumption is certainly valid in a wide range of sollicitation (e.g is consistent with the classical linearized elasticity), but must be somehow validated experimentally. Note that the complete model (50)–(53) can take into account the volumetric/deviatoric coupling which is relevant for high velocity impact [28]. Indeed, extreme strain-rate experiments can induced finite elastic deformations before plasticity occurs, so that pressure-dependent shear modulus are required (see for instance the SCG model [2, 33]).

### 3.4. Time derivative of the massic internal energy

The massic internal energy takes a rather elegant form:

$$\begin{aligned} e^m &= q_{exp}^{m(5)}(T) - \frac{1}{\rho_0} \int_{J_{exp}^{(5)}(T)}^J (p_{exp}^{(2)} - T \partial_T p_{exp}^{(2)})(T, \tilde{J}) d\tilde{J} + \frac{1}{\rho_0} \int_0^{\gamma_s} \left( \hat{\tau}_{exp}^{(3)} - T \partial_T \hat{\tau}_{exp}^{(3)} \right) (T, \tilde{\gamma}_s) d\tilde{\gamma}_s \\ &\quad + \frac{1}{\rho_0} \int_0^{\gamma_t} \frac{\gamma_s - \tau}{\sqrt{(\gamma_s - \tau)^2 - \gamma_s^2}} \left( \hat{\tau}_{exp}^{(4)} - T \partial_T \hat{\tau}_{exp}^{(4)} \right) (T, \gamma_s, \tau) d\tau. \end{aligned} \quad (58)$$

The time derivative of the internal energy, essential for the numerical implementation, is obtained by evaluating the partial derivatives of the massic internal energy with respect to its four variables (see Appendix E for details):

$$\frac{de^m}{dt} = \frac{\partial e^m}{\partial T} \dot{T} + \frac{\partial e^m}{\partial J} \dot{J} + \frac{\partial e^m}{\partial \gamma_s} \dot{\gamma}_s + \frac{\partial e^m}{\partial \gamma_t} \dot{\gamma}_t. \quad (59)$$

258 **4. Idealizations of elementary paths**

259 The expressions (50)–(53) yields the “exact” thermo-elastic behavior of an isotropic material and lies  
 260 upon four experimental results. In this section, we will propose physically consistent expressions for the  
 261 experimental stresses. We will see that some rather simple forms reduce our model to a few hyperelastic  
 262 models classically found in the literature.

263 *4.1. Pressure assumption*

264 **Hypothesis** Experimental pressure  $p_{exp}^{(2)}$ . We assume the following form for the pressure  $p_{exp}^{(2)}$  in any  
 265 isothermal spherical deformation:

$$p_{exp}^{(2)}(T, J) = p_{exp}^{(1)}(T) - \kappa(T) \ln J, \quad (60)$$

266 where  $p_{exp}^{(1)}(T)$  is the pressure from the path  $\mathcal{P}^{(1)}$

267  $\kappa(T)$  is a temperature-dependent bulk modulus.

The pressure (60) is reasonable (note for instance  $\lim_{J \rightarrow \infty} p_{exp}^{(2)} = -\infty$ ,  $\lim_{J \rightarrow 0} p_{exp}^{(2)} = \infty$ ), but predicts a finite strain energy under infinite compression  $J \rightarrow 0$ . For further details about the volumetric part of the Helmholtz free energy from which the pressure is derived, we refer to [12] and references therein. A more reasonable approximation of the experimental stress would be:

$$p_{exp}^{(2)} = p_{exp}^{(1)}(T) - \frac{\kappa(T)}{2} \left( J - \frac{1}{J} \right), \quad (61)$$

$$\Rightarrow g^{(2)}(T, J) = -\frac{(J-1)p_{exp}^{(1)}(T)}{\rho_0} + \frac{\kappa(T)}{2} \left( \frac{1}{2}(J^2 - 1) - \ln J \right). \quad (62)$$

268 It's worth noticing that (62) coincides with that proposed by [31] which is a variant of [8].

269 For the sake of calculus simplicity, we will however keep the pressure given by (60) for the following,  
 270 noting that the differences between (60) and (61) are very small for any volumic expansion up to 200%.

271 Both model comes down to the so called linearized elasticity when  $J \approx 1$  as  $\ln J \approx \frac{1}{2} \left( J - \frac{1}{J} \right) \approx \text{Tr} \boldsymbol{\varepsilon}$ .

272  $g^{(2)}$  is obtained using both (60) and (51):

$$g^{(2)}(T, J) = -\frac{(J-1)p_{exp}^{(1)}(T)}{\rho_0} + \frac{\kappa(T)}{\rho_0} (J \ln(J) + 1 - J). \quad (63)$$

273

274

275 If we replace the first path  $\mathcal{P}^{(1)}$  by a free expansion  $\mathcal{P}^{(5)}$  (in which one save  $q_{exp}^{m(5)}(T)$  and  $J_{exp}^{(5)}(T)$ )  
 276 followed by an isothermal spherical compression to bring  $J$  back to 1,  $p_{exp}^{(1)}(T)$  is obtained by evaluating (60)  
 277 in  $(T, J_{exp}^{(5)})$ . Remembering that the stress is zero in a freely expanded test, it comes:

$$p_{exp}^{(1)}(T) = \kappa(T) \ln \left( J_{exp}^{(5)}(T) \right). \quad (64)$$

278 Therefore, by reinjecting this expression (64) into the general formula (60), we deduce the expression of  
 279  $p_{exp}^{(2)}$ :

$$p_{exp}^{(2)}(T, J) = -\kappa(T) \ln \frac{J}{J_{exp}^{(5)}(T)}. \quad (65)$$

280 **Hypothesis** Free-stress volume expansion  $J_{exp}^{(5)}(T)$ . One can set arbitrary for  $J_{exp}^{(5)}(T)$ :

$$J_{exp}^{(5)}(T) = 1 + \beta(T - T_0), \quad (66)$$

281 where  $\beta$  refers to a free-stress expansion coefficient.

282 Inserting both the experimental pressure (64) and the free-stress volume expansion (66) in (63),  $g^{(2)}(T, J)$   
 283 now yields:

$$g^{(2)}(T, J) = \frac{\kappa(T)}{\rho_0} \left( J \ln \left( \frac{J}{1 + \beta(T - T_0)} \right) + 1 - J + \ln(1 + \beta(T - T_0)) \right). \quad (67)$$

284 4.2. Massic heat  $q_{exp}^{m(1)}$

285 As a reminder, the first path  $\mathcal{P}^{(1)}$  can be substituted by a free thermal expansion followed by isothermal  
 286 compression. We then obtain:

$$q_{exp}^{m(1)}(T) = q_{exp}^{m(5)}(T) + \frac{1}{\rho_0} \int_1^{J_{exp}^{(5)}} p_{exp}^{(2)}(T, \tilde{J}) - T \partial_T p_{exp}^{(2)}(T, \tilde{J}) d\tilde{J} \quad [see (44)]. \quad (68)$$

287 The conservation of energy in a free expansion is then written according to (65):

$$q_{exp}^{m(5)}(T) = q_{exp}^{m(1)}(T) + \frac{1}{\rho_0} \left( T \kappa(T) \frac{\partial_T J_{exp}^{(5)}}{J_{exp}^{(5)}} (J_{exp}^{(5)} - 1) + (\kappa(T) - T \kappa'(T)) (1 + \ln(J_{exp}^{(5)}) - J_{exp}^{(5)}) \right). \quad (69)$$

288 We can choose a simple function of  $q_{exp}^{m(5)}(T)$  or  $q_{exp}^{m(1)}(T)$  the other being determined by (69).

289 It is noteworthy that the idealizations of experimental curves presented in this section are only arbitrary  
 290 examples that have no theoretical justification.

291 **Hypothesis** Massic heat  $q_{exp}^{m(5)}(T)$ . A physically reasonable approximation to  $q_{exp}^{m(5)}(T)$  may be, for  
 292 example:

$$q_{exp}^{m(5)}(T) = C_p(T - T_0), \quad (70)$$

293 where  $C_p$  refers to a specific heat capacity in free expansion.

294 4.3. Calculation of  $g^{(3)}$

295 **Hypothesis** In-plane shear stress  $\hat{\tau}_{exp}^{(3)}$ . We assume that a temperature dependent simple shear modulus  
 296  $\mu(T)$  linearly links the shear stress with respect to the shear parameter  $\gamma$ :

$$\hat{\tau}_{exp}^{(3)}(T, J, \gamma) = \mu(T) \gamma. \quad (71)$$

297 The shear stress (71) leads to a quadratic massic free energy with respect to  $\gamma_s$  that is also independent of  
 298 the volume expansion  $J$ :

$$g^{(3)}(T, \gamma_s) = \frac{\mu(T)\gamma_s^2}{2\rho_0}. \quad (72)$$

299 This Helmholtz massic free energy has for example been postulated in [29]. We now choose to enhance the  
 300 model considering the contribution of the second invariant  $\bar{B}_{\text{II}}$  through  $\gamma_t$ .

#### 301 4.4. Calculation of $g^{(4)}$

302 The out-of-plane shear stress is a purely non-linear effect and its interpretation in terms of a ‘‘classical’’  
 303 shear or compressibility coefficient is therefore impossible.

304 **Hypothesis** Out-of-plane shear stress  $\hat{\tau}_{exp}^{(4)}$ . We postulate that the shear stress  $\hat{\tau}_{exp}^{(4)}$  in the fourth path  
 305  $\mathcal{P}^{(4)}$  is given by:

$$\hat{\tau}_{exp}^{(4)}(T, \gamma_s, \tau) = \alpha(T)\sqrt{(\gamma_s - \tau)^2 - \gamma_s^2}, \quad (73)$$

306  $\alpha(T)$  refers to a non-linear shear modulus. We further recall that the invariant  $\gamma_t$  is always negative during  
 307 the double shear test so that the square root involved in (73) is well-defined. Using the expression (73)  $g^{(4)}$   
 308 now reads:

$$g^{(4)}(T, \gamma_s, \gamma_t) = \frac{\alpha(T)}{\rho_0} \int_0^{\gamma_t} (\gamma_s - \tau) d\tau = \frac{\alpha(T)}{2\rho_0} (\gamma_s^2 - (\gamma_s - \gamma_t)^2). \quad (74)$$

#### 309 4.5. Idealized elastic law

310 With the idealizations of the experimental stresses (60), (71), (73) the  $g^{(\bullet)}$  functions were explicitly  
 311 calculated (63), (72), (74). The derivation of the Helmholtz free energy yields the current Cauchy stress:

$$\boldsymbol{\sigma} = \rho_0 \left( \partial_J \tilde{f}_\psi \mathbf{1} + \frac{1}{\gamma_s J^{\frac{5}{3}}} (\mu(T)\gamma_s + \alpha(T)(\gamma_s - \gamma_t)) \mathbf{Dev} \mathbf{B} + \frac{\alpha(T)}{J^{\frac{7}{3}}} \mathbf{Dev} (\mathbf{B}^2 - \text{Tr}(\mathbf{B})\mathbf{B}) \right). \quad (75)$$

312 The invariant  $\gamma_t$  is upper bounded by  $\gamma_s$  whereas the positivity of the second invariant  $J_2^B$  implies the lower  
 313 bound:

$$J_2^B = \sqrt{\frac{3}{2}} \|\mathbf{Dev} \mathbf{B}\| \geq 0 \Rightarrow \gamma_t \geq \gamma_s \left( 1 - \sqrt{\frac{1 + \gamma_s^2}{4}} \right). \quad (76)$$

314 Finally  $\lim_{\gamma_s \rightarrow 0} \frac{\gamma_t}{\gamma_s} = 0$  so that (75) does not diverge when  $\gamma_s \rightarrow 0$ . As we will see in the following section, the  
 315 expression (75) is algebraically equivalent to a standard Mooney-Rivlin model.

### 316 5. Analogy with the Mooney-Rivlin model

317 If we retain the idealizations (71), (73), the dependence of the massic free energy with respect to the  
 318 isochoric invariants is written:

$$\begin{aligned} g^{(3)}(T, \gamma_s) + g^{(4)}(T, \gamma_s, \gamma_t) &= \frac{1}{2\rho_0} (\mu(T)\gamma_s^2 + \alpha(T)(\gamma_s^2 - (\gamma_s - \gamma_t)^2)) \\ &= \frac{1}{2\rho_0} (\mu(T)(\bar{B}_{\text{I}} - 3) + \alpha(T)((\bar{B}_{\text{I}} - 3) - (\bar{B}_{\text{II}} - 3))). \end{aligned} \quad (77)$$

319 The right and left Cauchy-Green strain tensors  $\mathbf{C}$  and  $\mathbf{B}$  share their invariants  $B_i = C_i$ , as  $\mathbf{C}$  and  $\mathbf{B}$  are  
320 related through the rotation tensor  $\mathbf{R}$  arising from the polar decomposition of the transformation gradient  
321  $\mathbf{F} = \mathbf{R} \cdot \mathbf{U} = \mathbf{V} \cdot \mathbf{R}$ . Therefore the free energy (77) coincides exactly with that of a Mooney-Rivlin model  
322 [22]:

$$\psi_{M-R}^m = g^1(T) + g^2(T, J) + \frac{C_{01}}{\rho_0} (\bar{B}_I - 3) + \frac{C_{10}}{\rho_0} (\bar{B}_{II} - 3), \quad (78)$$

323 with the parameters  $C_{01} = \frac{1}{2}(\mu(T) + \alpha(T))$ ,  $C_{10} = -\frac{\alpha(T)}{2}$ .

324 If we assume that the shear stress along the  $\mathcal{P}^{(4)}$  path is identically zero, the massic free energy be-  
325 comes independent of the  $\gamma_t$  invariant and we then observe that the Helmholtz massic free energy evolves  
326 linearly with  $\bar{B}_I - 3$ , which corresponds to the Neo-Hookean model  $\psi_{N-H}^m = g^1(T) + g^2(T, J) + \frac{\mu}{2\rho_0} (\bar{B}_I - 3)$ .  
327 Consequently our thermodynamic approach includes these two models which result from the experimental  
328 idealizations (71) (73).

329  
330 More generally, if one looks at the in-plane shear stress curve  $\tau_{exp}^{(3)}$  as a function of the slip parameter  
331  $\gamma$ , it is certain that a polynomial expansion fitting experimental data can be found. By symmetry, this  
332 polynomial expansion must necessarily contain only even powers:

$$\hat{\tau}_{exp}^{(3)}(T, \gamma) = \sum_i \mu_i \gamma^{2i+1}. \quad (79)$$

333 (79) then generates a generalized Neo-Hookean model (power series of the free energy with respect to the  
334 “ $\bar{B}_I - 3$ ” invariant).

335 Moreover, if we postulate by the same reasoning that the out-of-plane shear stress  $\hat{\tau}_{exp}^{(4)}$  develops in the  
336 form:

$$\hat{\tau}_{exp}^{(3)}(T, \gamma) = \sum_i \mu_i \gamma^{2i+1} \text{ and } \hat{\tau}_{exp}^{(4)}(T, \gamma_s, \tau) = \sum_i \alpha_i \sqrt{(\gamma_s - \tau)^2 - \gamma_s^2} (\gamma_s - \tau)^{2i}. \quad (80)$$

337 Then one found the following Helmholtz massic free energy:

$$\begin{aligned} \psi^m &= \frac{1}{\rho_0} \sum_i \frac{\mu_i(T)}{2i+2} (\bar{B}_I - 3)^i + \frac{\alpha_i(T)}{2i+2} [(\bar{B}_I - 3)^i - (\bar{B}_{II} - 3)^i] + g^1(T) + g^2(T, J), \\ \psi^m &= \frac{1}{\rho_0} \sum_i C_{i0} (\bar{B}_I - 3)^i + C_{0i} (\bar{B}_{II} - 3)^i + g^1(T) + g^2(T, J) \quad C_{ij} = 0 \text{ if } i \neq j. \end{aligned} \quad (81)$$

338 That is, a generalized Mooney-Rivlin material [22].

339  
340 In the general case, the integral expressions given in section 3.2 yield the exact finite strain isotropic  
341 thermo-elastic constitutive law.

## 342 6. Conclusion

343 We have developed a complete finite-strain isotropic thermo-elastic model without any assumption con-  
344 cerning the form of the Helmholtz free energy. The identification of the latter relies on the successive

345 realization of four elementary experiments, and more precisely the measurement of: a massic heat, a pres-  
 346 sure, and two shear stresses. Experiments must be carried many times in order to scan all the accessible  
 347 values of the state variables e.g. the double shear test  $\mathcal{P}^{(4)}$  must be performed for a whole collection of  
 348 temperature  $T$ , volume expansion  $J$ , and slip  $\gamma_s$ .

349 Some idealizations of the experimental stresses have been proposed. They can be replaced by any realistic  
 350 curves, or even be given by the upscaling results of a large scale molecular dynamic simulation.

351 The well known Mooney-Rivlin model, and consequently the Neo-Hookean, are special cases of our  
 352 methodology. They are derived from an assumption concerning the shear stress along the  $\mathcal{P}^{(3)}$  and  $\mathcal{P}^{(4)}$   
 353 paths.

354 The present work could admit several natural extensions among which:

- 355 • The description of an anisotropic medium by the introduction of structural tensors  $\{\mathbf{N}_t^\bullet\}$  representing  
 356 the actual directions of anisotropy. Enhancing the Helmholtz free energy with these new unknowns  
 357 necessarily yields cross-invariant effects, reflecting the current orientation of the deformation with  
 358 respect to the anisotropic directions.
- 359 • A finite strain plasticity model with the addition of an objective plastic strain tensor  $\mathbf{B}^p$  in the  
 360 arguments' list of the Helmholtz free energy. Taking this tensor into account adds 6 state variables.  
 361 Three of them are specific to the plastic strain  $\mathbf{B}^p$  (2 if one further assumes that the plastic evolution  
 362 is isochoric), three others orient the principal directions orthogonal trihedron of  $\mathbf{B}$  and  $\mathbf{B}^p$ .
- 363 • The study of large-amplitude shock waves and more particularly shock tails. Indeed, after a large  
 364 plastic phase which is out of the scope of this study, the elastic release wave on the shock tail can be  
 365 considered as large strain. A proper coupling between both, an equation of state driving the pressure,  
 366 and the deviatoric elastic law presented herein is a very interesting perspective.

### 367 Acknowledgement

368 The author would like to thank his colleagues from the CEA for their fruitful remarks but also Pr. Jean  
 369 Guarrigues whose rigorous work gave rise to this article.

### 370 Appendix A. Justification of the finite strain isotropic elastic law

371 The definition of the Finger tensor is  $\mathbf{B} = \mathbf{F} \cdot \mathbf{F}^\top$ , hence its time derivative reads:

$$\begin{aligned} \dot{\mathbf{B}} &= \dot{\mathbf{F}} \cdot \mathbf{F}^\top + \mathbf{F} \cdot \dot{\mathbf{F}}^\top = (\dot{\mathbf{F}} \cdot \mathbf{F}^{-1}) \cdot (\mathbf{F} \cdot \mathbf{F}^\top) + (\mathbf{F} \cdot \mathbf{F}^\top) \cdot (\mathbf{F}^{-\top} \cdot \dot{\mathbf{F}}^\top), \\ \dot{\mathbf{B}} &= (\mathbf{D} + \mathbf{W}) \cdot \mathbf{B} + \mathbf{B} \cdot (\mathbf{D} - \mathbf{W}). \end{aligned} \tag{A.1}$$

372 where  $\mathbf{D}$  (resp  $\mathbf{W}$ ) denotes the symmetric (resp skew-symmetric) part of the spatial velocity gradient.

373 Using the combined product  $\mathbf{A}_1 : (\mathbf{A}_2 \cdot \mathbf{A}_3) = \mathbf{A}_2 : (\mathbf{A}_1 \cdot \mathbf{A}_3^\top) = \mathbf{A}_3 : (\mathbf{A}_2^\top \cdot \mathbf{A}_1)$ , we get successively,  
 374  $\forall n \in \mathbb{Z}$ :

$$\mathbf{B}^n : \dot{\mathbf{B}} = \mathbf{B}^n : ((\mathbf{D} + \mathbf{W}) \cdot \mathbf{B} + \mathbf{B} \cdot (\mathbf{D} - \mathbf{W})) = 2\mathbf{B}^{n+1} : \mathbf{D}. \quad (\text{A.2})$$

375 Orthogonality of the antisymmetric and symmetric tensors for the doubly contracted product has been used  
 376 to simplify (A.2).

377 The time derivatives of the coefficients of the characteristic polynomials of  $\mathbf{B}$  are (see also [14, 15]):

$$\begin{aligned} \frac{dB_I}{dt} &= \text{Tr} \frac{d\mathbf{B}}{dt} = \mathbf{1} : \dot{\mathbf{B}}; & \frac{dB_{II}}{dt} &= (B_I \mathbf{1} - \mathbf{B}^\top) : \frac{d\mathbf{B}}{dt}; & \frac{dB_{III}}{dt} &= (B_{II} \mathbf{1} - B_I \mathbf{B}^\top + \mathbf{B}^{2\top}) : \frac{d\mathbf{B}}{dt} = B_{III} \mathbf{B}^{-\top} : \frac{d\mathbf{B}}{dt}; \\ \dot{B}_I &= 2\mathbf{B} : \mathbf{D}; & \dot{B}_{II} &= 2(B_I \mathbf{B} - \mathbf{B}^2) : \mathbf{D}; & \dot{B}_{III} &= B_{III} \mathbf{1} : \mathbf{D}; \end{aligned} \quad (\text{A.3})$$

378 The nullity of intrinsic dissipation (4), is written using the coincident isotropic function (5):

$$-\rho \left( \partial_T f_\psi^B \dot{T} + \partial_{B_I} f_\psi^B \dot{B}_I + \partial_{B_{II}} f_\psi^B \dot{B}_{II} + \partial_{B_{III}} f_\psi^B \dot{B}_{III} + \dot{T} s^m \right) + \boldsymbol{\sigma} : \mathbf{D} = 0. \quad (\text{A.4})$$

379 Injecting both (A.3), (A.2) in (A.4) and using the fact that  $\boldsymbol{\sigma}$  and  $f_\psi^B$  are state functions so that they do  
 380 not depend on  $\mathbf{D}$ , the nullity of (A.4)  $\forall T \forall \mathbf{D}$  yields the elastic law (6).

### 381 Appendix B. Thermo-elastic law with respect to isochoric invariants

382 The partial derivatives of the new function  $\tilde{f}_\psi^B$  defined by (11) are simple algebraic calculations:

$$\begin{aligned} \partial_{B_I} f_\psi^B &= \partial_{\bar{B}_I} \tilde{f}_\psi^B \partial_{B_I} \bar{B}_I = B_{III}^{-\frac{1}{3}} \partial_{\bar{B}_I} \tilde{f}_\psi^B, \\ \partial_{B_{II}} f_\psi^B &= \partial_{\bar{B}_{II}} \tilde{f}_\psi^B \partial_{B_{II}} \bar{B}_{II} = B_{III}^{-\frac{2}{3}} \partial_{\bar{B}_{II}} \tilde{f}_\psi^B, \\ \partial_{B_{III}} f_\psi^B &= \partial_{\bar{B}_I} \tilde{f}_\psi^B \partial_{B_{III}} \bar{B}_I + \partial_{\bar{B}_{II}} \tilde{f}_\psi^B \partial_{B_{III}} \bar{B}_{II} + \partial_{B_{III}} \tilde{f}_\psi^B, \\ \partial_{B_{III}} f_\psi^B &= -\partial_{\bar{B}_I} \tilde{f}_\psi^B \frac{\bar{B}_I}{3B_{III}} - \partial_{\bar{B}_{II}} \tilde{f}_\psi^B \frac{2\bar{B}_{II}}{3B_{III}} + \partial_{B_{III}} \tilde{f}_\psi^B. \end{aligned} \quad (\text{B.1})$$

383 And the elastic law (6) now reads:

$$\begin{aligned} \boldsymbol{\sigma} &= \frac{2\rho_0}{\sqrt{B_{III}}} \left( \left( B_{III} \partial_{B_{III}} \tilde{f}_\psi^B - \partial_{\bar{B}_I} \tilde{f}_\psi^B \frac{\bar{B}_I}{3} - \partial_{\bar{B}_{II}} \tilde{f}_\psi^B \frac{2\bar{B}_{II}}{3} \right) \mathbf{1} \right. \\ &\quad \left. + \left( B_{III}^{-\frac{1}{3}} \partial_{\bar{B}_I} \tilde{f}_\psi^B + B_{III}^{\frac{1}{3}} \bar{B}_I B_{III}^{-\frac{2}{3}} \partial_{\bar{B}_{II}} \tilde{f}_\psi^B \right) \mathbf{B} - B_{III}^{-\frac{2}{3}} \partial_{\bar{B}_{II}} \tilde{f}_\psi^B \mathbf{B}^2 \right), \\ \boldsymbol{\sigma} &= \frac{2\rho_0}{\sqrt{B_{III}}} \left( \left( B_{III} \partial_{B_{III}} \tilde{f}_\psi^B - \partial_{\bar{B}_I} \tilde{f}_\psi^B \frac{\bar{B}_I}{3} - \partial_{\bar{B}_{II}} \tilde{f}_\psi^B \frac{2\bar{B}_{II}}{3} \right) \mathbf{1} \right. \\ &\quad \left. + \left( \partial_{\bar{B}_I} \tilde{f}_\psi^B + \bar{B}_I \partial_{\bar{B}_{II}} \tilde{f}_\psi^B \right) \bar{\mathbf{B}} - \partial_{\bar{B}_{II}} \tilde{f}_\psi^B \bar{\mathbf{B}}^2 \right). \end{aligned} \quad (\text{B.2})$$

384 This formula is more elegantly written using the following relations, which hold for any tensor of order 2:

$$\begin{aligned} X_{II} = \frac{1}{2} (X_I^2 - \text{Tr} \mathbf{X}^2) &\Rightarrow -\frac{2}{3} X_{II} \mathbf{1} + X_I \mathbf{X} - \mathbf{X}^2 = -\frac{1}{3} (X_I^2 - \text{Tr} \mathbf{X}^2) \mathbf{1} + X_I \mathbf{X} - \mathbf{X}^2, \\ &= -\text{Dev} (\mathbf{X}^2 - \text{Tr} (\mathbf{X}) \mathbf{X}). \end{aligned} \quad (\text{B.3})$$

385 So that (B.2) is finally written:

$$\begin{aligned}\sigma &= \frac{2\rho_0}{\sqrt{B_{\text{III}}}} \left( B_{\text{III}} \partial_{B_{\text{III}}} \tilde{f}_\psi^B \mathbf{1} + \partial_{\bar{B}_I} \tilde{f}_\psi^B \text{Dev} \bar{\mathbf{B}} - \partial_{\bar{B}_{\text{II}}} \tilde{f}_\psi^B \text{Dev} \left( \bar{\mathbf{B}}^2 - \text{Tr}(\bar{\mathbf{B}}) \bar{\mathbf{B}} \right) \right), \\ \sigma &= \frac{2\rho_0}{\sqrt{B_{\text{III}}}} \left( B_{\text{III}} \partial_{B_{\text{III}}} \tilde{f}_\psi^B \mathbf{1} + \frac{\partial_{\bar{B}_I} \tilde{f}_\psi^B}{B_{\text{III}}^{\frac{1}{3}}} \text{Dev} \mathbf{B} - \frac{\partial_{\bar{B}_{\text{II}}} \tilde{f}_\psi^B}{B_{\text{III}}^{\frac{2}{3}}} \text{Dev} \left( \mathbf{B}^2 - \text{Tr}(\mathbf{B}) \mathbf{B} \right) \right).\end{aligned}\quad (\text{B.4})$$

### 386 Appendix C. Evolution domain of $\gamma_t$

Let  $(\bar{\lambda}_i)_{i \in [1,3]}$  be the principal stretches of the isochoric Finger tensor  $\bar{\mathbf{B}}$ . We further assume that the invariant  $\gamma_s$  remains fixed. The following system is necessarily verified by the triplet  $(\bar{\lambda}_i)_{i \in [1,3]}$ :

$$\bar{\lambda}_1^2 + \bar{\lambda}_2^2 + \bar{\lambda}_3^2 = \gamma_s^2 + 3 = \bar{B}_I, \quad (\text{C.1})$$

$$\bar{\lambda}_1^2 \bar{\lambda}_2^2 + \bar{\lambda}_2^2 \bar{\lambda}_3^2 + \bar{\lambda}_1^2 \bar{\lambda}_3^2 = \bar{B}_{\text{II}}, \quad (\text{C.2})$$

$$\bar{\lambda}_1 \bar{\lambda}_2 \bar{\lambda}_3 = 1. \quad (\text{C.3})$$

387 By combining the equations (C.1) and (C.3), we deduce:

$$\bar{\lambda}_2^4 + \left( \bar{\lambda}_1^2 - \bar{B}_I \right) \bar{\lambda}_2^2 + \frac{1}{\bar{\lambda}_1^2} = 0. \quad (\text{C.4})$$

388 (C.4) has a positive or zero discriminant:

$$\Delta = \left( \bar{\lambda}_1^2 - \bar{B}_I \right)^2 - \frac{4}{\bar{\lambda}_1^2} \geq 0 \Rightarrow \bar{\lambda}_{2\pm} = \frac{\bar{B}_I - \bar{\lambda}_1^2 \pm \sqrt{\left( \bar{\lambda}_1^2 - \bar{B}_I - \frac{2}{\bar{\lambda}_1} \right) \left( \bar{\lambda}_1^2 - \bar{B}_I + \frac{2}{\bar{\lambda}_1} \right)}}{2}. \quad (\text{C.5})$$

389 The positivity of the term under the square root implies that (C.4) has real solutions if and only if the  
390 eigenvalue  $\bar{\lambda}_1$  evolves in the interval:

$$\bar{\lambda} \in [X_2, X_0] \text{ with } X_k = 3\sqrt{\tilde{\alpha}} \cos \left( \frac{1}{3} \arccos \left( -(\tilde{\alpha})^{-\frac{3}{2}} \right) + \frac{2k\pi}{3} \right) \text{ with } \tilde{\alpha} = \frac{\bar{B}_I}{3} \geq 0. \quad (\text{C.6})$$

391 We can then express  $\gamma_t$  as a function of the unique variable  $\bar{\lambda}_1$ :

$$\bar{B}_{\text{II}}(\bar{\lambda}_1) = \bar{\lambda}_1^2 \bar{\lambda}_{2\pm}^2 + \frac{1}{\bar{\lambda}_1^2} + \frac{1}{\bar{\lambda}_{2\pm}^2} = \bar{\lambda}_1^2 \bar{B}_I - \bar{\lambda}_1^4 + \frac{1}{\bar{\lambda}_1^2} \Rightarrow \gamma_t(\bar{\lambda}_1) = \gamma_s - \sqrt{\bar{B}_{\text{II}}(\bar{\lambda}_1) - 3} \quad (\text{C.7})$$

392 Fixing  $\gamma_s$  successively, we plot the evolution domain of  $\gamma_t$  (see Figure C.3a) and compare it to the set that  
393 can be scanned by the double shear test:

$$\gamma_t \in \left[ \gamma_s \left( 1 - \sqrt{1 + \frac{\gamma_s^2}{4}} \right), 0 \right]. \quad (\text{C.8})$$

394 Some values of the shear parameter  $\gamma_t$  are not accessible through the double shear test (see Figure C.3b).  
395 Therefore, we present in the following Appendix D a more general motion which scan the whole domain of  
396 variation for  $\gamma_t$ .

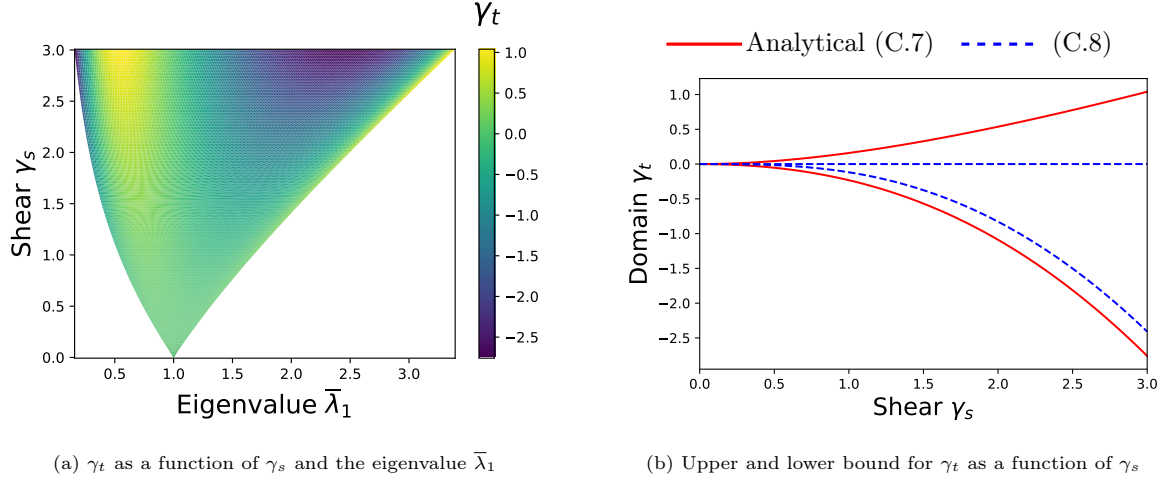


Figure C.3: Value of the second invariant  $\gamma_t$  for various  $\gamma_s$

### 397 Appendix D. Double shear traction

398 We define as “isochoric double shear-traction test” the motion given by the following gradient:

$$\mathbf{F} = J^{\frac{1}{3}} \begin{pmatrix} \frac{1}{\sqrt{e}} & \gamma & 0 \\ 0 & \frac{1}{\sqrt{e}} & \gamma_{\perp} \\ 0 & 0 & e \end{pmatrix} \Rightarrow \bar{\mathbf{B}} = \begin{pmatrix} \frac{1}{e} + \gamma^2 & \frac{\gamma}{\sqrt{e}} & 0 \\ & \frac{1}{e} + \gamma_{\perp}^2 & \gamma_{\perp} e \\ Sym & & e^2 \end{pmatrix}. \quad (\text{D.1})$$

399 The “double shear test” mentioned in Section 3.1.4 corresponds to  $e = 1$ . We also denote as “simple tensile-  
400 shear test” the case  $\gamma_{\perp} = 0$ .

401 The square of the Finger isochoric strain tensor is equal to:

$$\bar{\mathbf{B}}^2 = \begin{pmatrix} \left( \frac{1}{e} + \gamma^2 \right)^2 + \frac{\gamma^2}{e} & \frac{\gamma}{\sqrt{e}} \left( \frac{2}{e} + \gamma^2 + \gamma_{\perp}^2 \right) & \gamma_{\perp} \sqrt{e} \\ & \frac{\gamma^2}{e} + (\gamma_{\perp} e)^2 + \left( \frac{1}{e} + \gamma_{\perp}^2 \right)^2 & \gamma_{\perp} e \left( \frac{1}{e} + \gamma_{\perp}^2 + e^2 \right) \\ Sym & & (\gamma_{\perp} e)^2 + e^4 \end{pmatrix}. \quad (\text{D.2})$$

402 It’s worth noticing a non-zero  $\bar{B}_{13}^2$  deformation which induces a purely non-linear stress. This out-of plane  
403 shear stress is relevant for identifying the dependence of the free energy on the second invariant  $\gamma_t$ .

404 A simple computation of the characteristic polynomial of the isochoric Finger tensor shows that the  
405 fundamental invariants are equal to:

$$\bar{B}_I = \gamma^2 + \gamma_{\perp}^2 + e^2 + \frac{2}{e} \text{ and } \bar{B}_{II} = \gamma^2 (\gamma_{\perp}^2 + e^2) + 2e + \frac{1}{e^2} + \frac{\gamma_{\perp}^2}{e^2}. \quad (\text{D.3})$$

406 The conservation of the parameter  $\gamma_s$  is ensured if at each instant, the following equality holds:

$$\bar{B}_I = \gamma^2 + \gamma_{\perp}^2 + e^2 + \frac{2}{e} = \gamma_s^2 + 3 \text{ with } e(0) = 1, \gamma(0) = \gamma_s, \gamma_{\perp}(0) = 0. \quad (\text{D.4})$$

407 The motion has two independent parameters: a shear  $\gamma_\perp$  and a traction magnitude  $e$ . The value of  $\gamma$  is  
 408 adjusted so as to guarantee at each instant the equality (D.4).

409 We then deduce, by simple calculations, the value of the invariant  $\gamma_t$ :

$$\gamma_t(e, \gamma_\perp) = \gamma_s - \sqrt{(\gamma_\perp^2 + e^2) \left( \bar{B}_I - \gamma_\perp^2 - e^2 - \frac{2}{e} \right) + \frac{1}{e^2} + 2e + \frac{\gamma_\perp^2}{e} - 3}, \quad (\text{D.5})$$

410 with the necessary conditions of existence:

$$\bar{B}_I - \gamma_\perp^2 - e^2 - \frac{2}{e} \geq 0 \text{ and } e > 0. \quad (\text{D.6})$$

411 The existence conditions (D.6) define a sub-domain of  $\mathbb{R}^2$ . At  $\gamma_\perp \leq \gamma_s$  fixed, the range of variation of  $e$   
 412 is analytic and simply given by  $e \in [e_2, e_0]$  with:

$$e_k = 2\sqrt{\tilde{\alpha}} \cos \left( \frac{1}{3} \arccos \left( -(\tilde{\alpha})^{-\frac{3}{2}} \right) + \frac{2k\pi}{3} \right) \text{ with } \tilde{\alpha} = \frac{\bar{B}_I - \gamma_\perp^2}{3} \geq 0. \quad (\text{D.7})$$

413 Hence, the values of the parameter  $\gamma_t$  that can be scanned through the simple shear tensile test ((D.9) with  
 414  $\gamma_\perp = 0$ ) are:

$$\begin{aligned} \gamma_t(e, 0) &= \gamma_s - \sqrt{e^2 \left( \bar{B}_I - e^2 - \frac{2}{e} \right) + \frac{1}{e^2} + 2e} \\ \gamma_t(e, 0) &= \gamma_s - \sqrt{e^2 \bar{B}_I - e^4 + \frac{1}{e^2}} \end{aligned} \quad e \in [e_2(0), e_0(0)], \quad e_k(0) \text{ given by (D.7)}. \quad (\text{D.8})$$

415 Whereas for the double-shear test ((D.9) with  $e = 1$ ):

$$\gamma_t(1, \gamma_\perp) = \gamma_s - \sqrt{(\gamma_\perp^2 + 1) (\bar{B}_I - \gamma_\perp^2 - 3) + \gamma_\perp^2} = \gamma_s - \sqrt{\gamma_s^2 + \gamma_\perp^2 (\gamma_s^2 - \gamma_\perp^2)}. \quad (\text{D.9})$$

416 We represent in figure D.4 the values of  $\gamma_t$  covered by the double shear tensile test with  $\gamma_s = 3$ . The red line  
 417 corresponds to the single tensile-shear test ( $\gamma_\perp = 0$ ), while the orange line corresponds to the double shear  
 418 test ( $e = 1$ ). The widest  $\gamma_t$  interval is scanned when  $\gamma_\perp = 0$  (see D.4), i.e., during a single tensile-shear test.

419  
 420 We further represent the  $\gamma_t$  that can be scanned by both the tensile-shear (Figure (D.5b)) and double  
 421 shear (Figure D.5a) tests for various  $\gamma_s$ . We note that the double-shear test only explores negative values of  
 422  $\gamma_t$  while the tensile-shear test scans the whole domain (see Figure D.6 or more simply the equality between  
 423 (C.7) and (D.8) as  $e = \bar{\lambda}_1$ ).

424  
 425 The identification of the constitutive law with respect to the second invariant  $\gamma_t$  Section 3.1.4 was built  
 426 upon the double shear test. The reason is quite simple: the single shear tensile test, although scanning the  
 427 whole domain for  $\gamma_t$ , does not allow to simply identify the dependence on  $\gamma_t$  because the non-linear stress  $\sigma_{13}$   
 428 vanishes. Therefore, measuring either  $\sigma_{12}$  or  $\sigma_{13}$  will couple  $g^{(4)}$  to the other functions. The most efficient  
 429 test, but also the hardest to perform experimentally, shall set a small shear strain  $\gamma_\perp$  and then perform a  
 430 tensile test by varying  $e$ . Hence  $\sigma_{13}$  would be non-zero and one could characterize  $\tilde{f}_\psi$  for  $\gamma_t \geq 0$ .

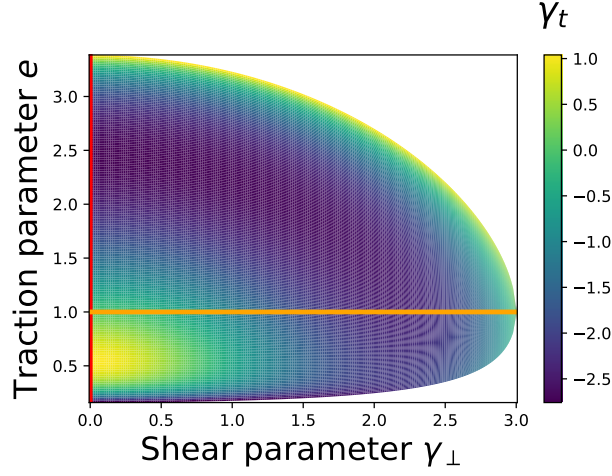


Figure D.4: Value of  $\gamma_t, \gamma_s = 3$  fixed, for different values of  $e$  and  $\gamma_\perp$

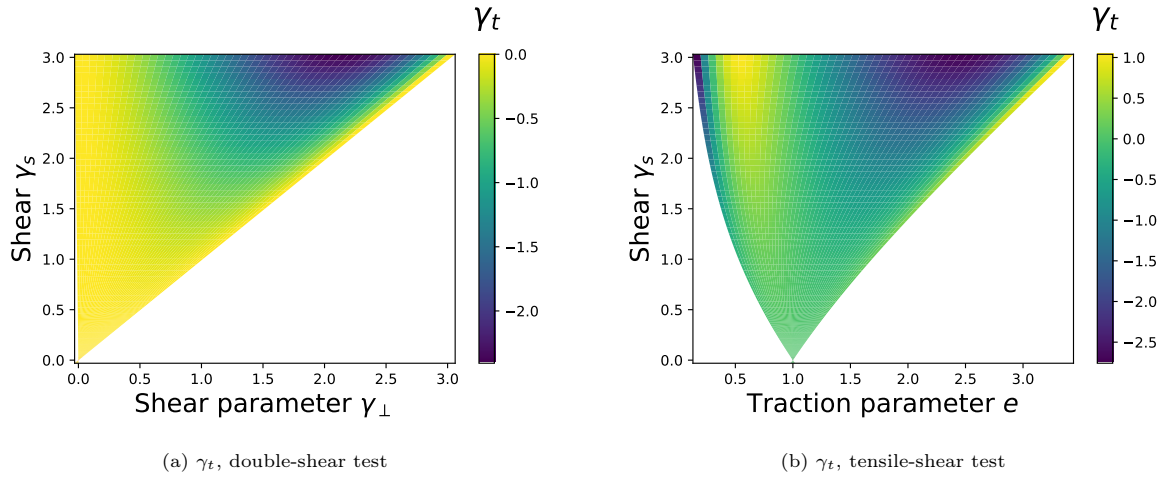


Figure D.5:  $\gamma_t$  for various  $\gamma_s$

#### 431 Appendix E. Generic partial derivatives of the internal energy

432 The partial derivative with respect to temperature is certainly the most cumbersome:

$$\begin{aligned}
 \frac{\partial e^m}{\partial T} &= \frac{dq_{exp}^{m(5)}}{dT} - \frac{1}{\rho_0} \frac{dJ_{exp}^{(5)}(T)}{dT} T \partial_T p_{exp}^{(2)}(T, J_{exp}^{(5)}(T)) \\
 &+ \frac{1}{\rho_0} \int_1^J T \partial_T^2 p_{exp}^{(2)}(T, \tilde{J}) d\tilde{J} - \frac{1}{\rho_0} \int_0^{\gamma_s} T \partial_T^2 \hat{\tau}_{exp}^{(3)}(T, \tilde{\gamma}_s) d\tilde{\gamma}_s \\
 &- \frac{1}{\rho_0} \int_0^{\gamma_t} \frac{\gamma_s - \tau}{\sqrt{(\gamma_s - \tau)^2 - \gamma_s^2}} T \partial_T^2 \hat{\tau}_{exp}^{(4)}(T, \gamma_s, \tau) d\tau.
 \end{aligned} \tag{E.1}$$

433 The partial derivative with respect to the volume expansion  $J$  thanks to the volumetric/isochoric split:

$$\frac{\partial e^m}{\partial J} = -\frac{1}{\rho_0} \left( p_{exp}^{(2)}(T, J) - T \partial_T p_{exp}^{(2)}(T, J) \right). \tag{E.2}$$

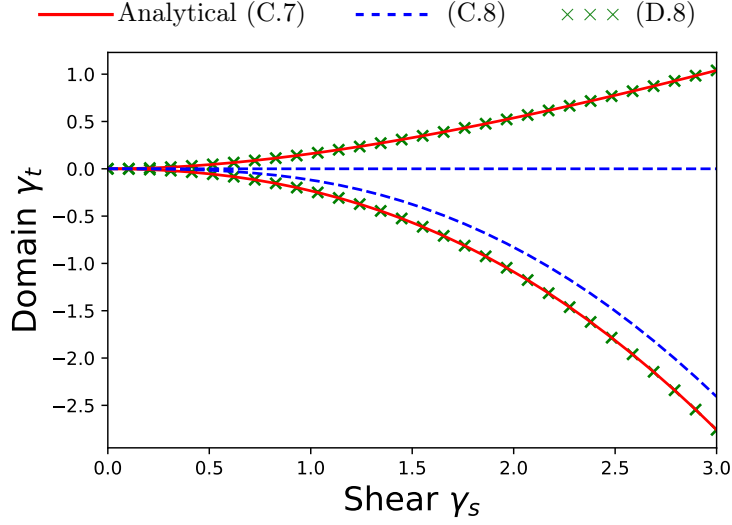


Figure D.6: Upper and lower bound of  $\gamma_t$

434 The partial derivative with respect to  $\gamma_s$  and  $\gamma_t$  are written as:

$$\begin{aligned} \frac{\partial e^m}{\partial \gamma_s} &= \frac{1}{\rho_0} \left( \hat{\tau}_{exp}^{(3)}(T, \gamma_s) - T \partial_T \hat{\tau}_{exp}^{(3)}(T, \gamma_s) \right) + \frac{1}{\rho_0} \int_0^{\gamma_t} \partial_{\gamma_s} \left( \frac{\gamma_s - \tau}{\sqrt{(\gamma_s - \tau)^2 - \gamma_s^2}} \left( \hat{\tau}_{exp}^{(4)} - T \partial_T \hat{\tau}_{exp}^{(4)} \right) (T, \gamma_s, \tau) \right) d\tau, \\ \frac{\partial e^m}{\partial \gamma_t} &= \frac{1}{\rho_0} \frac{\gamma_s - \gamma_t}{\sqrt{(\gamma_s - \gamma_t)^2 - \gamma_s^2}} \left( \hat{\tau}_{exp}^{(4)} - T \partial_T \hat{\tau}_{exp}^{(4)} \right) (T, \gamma_s, \gamma_t). \end{aligned} \quad (\text{E.3})$$

## 435 References

- 436 [1] J. Akella, G. Smith, R. Grover, Y. Wu, and S. Martin. Static eos of uranium to 100 gpa pressure. *High Pressure Research*,  
437 2(5-6):295–302, 1990.
- 438 [2] B. Banerjee. An evaluation of plastic flow stress models for the simulation of high-temperature and high-strain-rate  
439 deformation of metals. *arXiv preprint cond-mat/0512466*, 2005.
- 440 [3] M. A. Biot. Thermoelasticity and irreversible thermodynamics. *Journal of Applied Physics*, 27(3):240–253, 1956.
- 441 [4] J. Boehler. On irreducible representations for isotropic scalar functions. *ZAMM-Journal of Applied Mathematics and*  
442 *Mechanics/Zeitschrift für Angewandte Mathematik und Mechanik*, 57(6):323–327, 1977.
- 443 [5] J.-P. Boehler. A simple derivation of representations for non-polynomial constitutive equations in some cases of anisotropy.  
444 *ZAMM-Journal of Applied Mathematics and Mechanics/Zeitschrift für Angewandte Mathematik und Mechanik*, 59(4):  
445 157–167, 1979.
- 446 [6] J. Cassels, N. Hitchin, et al. *Nonlinear elasticity: theory and applications*. 2001.
- 447 [7] G. Chagnon, M. Rebouah, and D. Favier. Hyperelastic energy densities for soft biological tissues: a review. *Journal of*  
448 *Elasticity*, 120(2):129–160, 2015.
- 449 [8] P. G. Ciarlet. *Mathematical elasticity: Three-dimensional elasticity*. SIAM, 2021.
- 450 [9] B. D. Coleman and W. Noll. The thermodynamics of elastic materials with heat conduction and viscosity. In *The*  
451 *foundations of mechanics and thermodynamics*, pages 145–156. Springer, 1974.

- 452 [10] H. Dal, Y. Badienia, K. Açıkgöz, and F. A. Denli. A comparative study on hyperelastic constitutive models on rubber:  
453 State of the art after 2006. *Constitutive Models for Rubber XI*, pages 239–244, 2019.
- 454 [11] M. Dalem. *Une experimentation reussie pour l'identification de la reponse mecanique sans loi de comportement: Ap-  
455 proche data-driven appliquee aux membranes elastomeres*. PhD thesis, ecole centrale de Nantes, 2019.
- 456 [12] S. Doll and K. Schweizerhof. On the development of volumetric strain energy functions. *J. Appl. Mech.*, 67(1):17–21,  
457 2000.
- 458 [13] P. Flory. Thermodynamic relations for high elastic materials. *Transactions of the Faraday Society*, 57:829–838, 1961.
- 459 [14] J. Garrigues. *Algèbre et analyse tensorielles pour l'étude des milieux continus*. 2016.
- 460 [15] J. Garrigues. *Cinématique des milieux continus*, 2016.
- 461 [16] J. Garrigues. *Comportement élastique*, 2017.
- 462 [17] J. Garrigues. *Comportements inélastiques*, 2018.
- 463 [18] C. G'sell, S. Boni, and S. Shrivastava. Application of the plane simple shear test for determination of the plastic behaviour  
464 of solid polymers at large strains. *Journal of Materials Science*, 18(3):903–918, 1983.
- 465 [19] H. B. Khaniki, M. H. Ghayesh, R. Chin, and M. Amabili. A review on the nonlinear dynamics of hyperelastic structures.  
466 *Nonlinear Dynamics*, pages 1–32, 2022.
- 467 [20] B. Kim, S. B. Lee, J. Lee, S. Cho, H. Park, S. Yeom, and S. H. Park. A comparison among neo-hookean model, mooney-  
468 rivlin model, and ogden model for chloroprene rubber. *International Journal of Precision Engineering and Manufacturing*,  
469 13(5):759–764, 2012.
- 470 [21] S. Korobeynikov. Objective tensor rates and applications in formulation of hyperelastic relations. *Journal of Elasticity*,  
471 93(2):105–140, 2008.
- 472 [22] N. Kumar and V. V. Rao. Hyperelastic mooney-rivlin model: determination and physical interpretation of material  
473 constants. *Parameters*, 2(10):01, 2016.
- 474 [23] S. K. Melly, L. Liu, Y. Liu, and J. Leng. A review on material models for isotropic hyperelasticity. *International Journal  
475 of Mechanical System Dynamics*, 1(1):71–88, 2021.
- 476 [24] C. Miehe. Entropic thermoelasticity at finite strains. aspects of the formulation and numerical implementation. *Computer  
477 Methods in Applied Mechanics and Engineering*, 120(3-4):243–269, 1995.
- 478 [25] R. W. Ogden. *Non-linear elastic deformations*. Courier Corporation, 1997.
- 479 [26] J. Pamin, B. Wcisło, and K. Kowalczyk-Gajewska. Gradient-enhanced large strain thermoplasticity with automatic  
480 linearization and localization simulations. *Journal of Mechanics of Materials and Structures*, 12(1):123–146, 2016.
- 481 [27] C. Sansour. On the physical assumptions underlying the volumetric-isochoric split and the case of anisotropy. *European  
482 Journal of Mechanics-A/Solids*, 27(1):28–39, 2008.
- 483 [28] M. Scheidler. On the coupling of pressure and deviatoric stress in hyperelastic materials. In *Proceedings of the 13th Army  
484 Symposium on Solid Mechanics*, pages 539–550, 1993.
- 485 [29] J. Simo and C. Miehe. Associative coupled thermoplasticity at finite strains: Formulation, numerical analysis and imple-  
486 mentation. *Computer Methods in Applied Mechanics and Engineering*, 98(1):41–104, 1992.
- 487 [30] J. Simo, R. L. Taylor, and K. Pister. Variational and projection methods for the volume constraint in finite deformation  
488 elasto-plasticity. *Computer Methods in Applied Mechanics and Engineering*, 51(1-3):177–208, 1985.
- 489 [31] J. C. Simo and T. J. Hughes. *Computational inelasticity*, volume 7. Springer Science & Business Media, 2006.
- 490 [32] G. Smith. On isotropic functions of symmetric tensors, skew-symmetric tensors and vectors. *International Journal of  
491 Engineering Science*, 9(10):899–916, 1971.
- 492 [33] D. Steinberg, S. Cochran, and M. Guinan. A constitutive model for metals applicable at high-strain rate. *Journal of  
493 Applied Physics*, 51(3):1498–1504, 1980.
- 494 [34] D. Stewart. A platform with six degrees of freedom. *Proceedings of the institution of mechanical engineers*, 180(1):

- 495 371–386, 1965.
- 496 [35] C. Truesdell and W. Noll. The non-linear field theories of mechanics. In *The non-linear field theories of mechanics*, pages  
497 1–579. Springer, 2004.
- 498 [36] O. H. Yeoh. Some forms of the strain energy function for rubber. *Rubber Chemistry and Technology*, 66(5):754–771, 1993.
- 499 [37] Q.-S. Zheng and A. Spencer. Tensors which characterize anisotropies. *International Journal of Engineering Science*, 31  
500 (5):679–693, 1993.